Electronic Supporting Information to:

Conformational Design Concepts for Anions in Ionic Liquids

Frederik Philippi, [a] David Pugh, [a,b] Daniel Rauber, [c] Tom Welton, [a] and Patricia A. Hunt *[a]

a. Department of Chemistry, Molecular Sciences Research Hub, Imperial College London, White City Campus, London W12 0BZ, United Kingdom.

b. Department of Chemistry, Britannia House, 7 Trinity Street, London SE1 1DB, United Kingdom.

c. Department of Chemistry, Saarland University, 66123, Saarbrücken, Germany

Contents

1. Additional syntheses and crystal growth

1.1 N-(methylsulfonyl)acetamide [H][N(Ms)(Ac)]

[H][N(Ms)(Ac)] was synthesized via a modification of the literature route.[1] Methanesulfonamide (4.48 g, 47.0 mmol) was dissolved in MeCN (70 mL) under an inert atmosphere. Acetic anhydride (6.7 mL, 70.5 mmol) was added dropwise, followed by concentrated H_2SO_4 (136 mg, 1.4 mmol) and the reaction was stirred at 60 °C for 16 hours. After this time the reaction was cooled and volatiles removed *in vacuo*. Water (15 mL) was added then the reaction was extracted with Et_2O (3 x 50 mL). The organic fractions were combined, dried ($MgSO_4$), filtered and concentrated to dryness. The title compound was isolated as a white solid (5.73 g, 89% yield). Crystals were obtained by recrystallization from hot Et_2O.

1.2 Tetramethylammonium bis(trifluoromethylsulfonyl)methanide [NMe_4][$CH(Tf)_2$]

415 mg Methylene ditriflone (1.48 mmol / 1.01 eq) were dissolved in 3 mL water + 3 mL MeOH and cooled to 0°C. To the resulting suspension were added 616 µL tetramethylammonium hydroxide solution 25% (133 mg / 1.46 mmol / 1.00 eq) in methanol. The reaction mixture was stirred until homogeneous, and then dried in high vacuum to yield 522 mg of the title compound (1.47 mmol / qualtitative yield). Crystals were obtained by slow evaporation of a solution in methylene chloride. Commercially available methylene ditriflone (ABCR, Karlsruhe, Germany) should be resublimed prior to its use.

1.3 N-((trifluoromethyl)sulfonyl)acetamide [H][N(Tf)(Ac)]

Crystals of [H][N(Tf)(Ac)] were obtained interdiffusion of Hexane (antisolvent) into a solution of the free acid in diethyl ether (solvent) at 4°C.

1.4 Potassium acetyl(trifluoromethylsulfonyl) amide [K][N(Tf)(Ac)]

[K][N(Tf)(Ac)] was prepared analogous to [Na][N(Tf)(Ac)] in the main paper, using potassium hydrogen carbonate as base. Crystals were obtained from interdiffusion of diethyl ether (antisolvent) into a solution of the potassium salt in acetonitrile (solvent) at 4°C.

1.5 2,2,2-trifluoro-N-(methylsulfonyl)acetamide [H][N(Ms)(TFA)]

Crystals of [H][N(Ms)(TFA)] were obtained by slow evaporation from acetonitrile.

2. Crystallography

Datasets were collected using an Oxford Diffraction Xcalibur 3E (Mo K_α radiation, 0.71073 Å) at 173.0(1) K. Data processing was carried out using CrysAlisPro,[2] solutions were solved and refined using SHELX-97 and SHELXTL,[3] as well as Olex-2,[4] and WinGX.[5] Hydrogen atoms bonded to carbon were placed in geometrically assigned positions with C–H distances of 0.98 Å (CH_3) and refined using a riding model, with U_{iso}(H) = 1.5 U_{eq}(C) (CH_3). Hydrogen atoms bonded to nitrogen were added as idealised protons. CCDC reference numbers 1981615 ([H][N(Tf)(Ac)]), 1981616 ([K][N(Tf)(Ac)]), 1981617 ([H][N(Ms)(TFA)]), 1981618 ([H][N(Ms)(Ac)]) and 1981619 ([NMe_4][$CH(Tf)_2$]) contain crystallographic data in CIF format, which is also summarized below, Table 1.

HNMsTFA was modelled as a two component twin in a ca. 47:53 ratio, with the two major lattices related by the approximate twin law [-1.00 0.00 0.00 0.00 -1.00 0.00 0.30 0.01 1.00]. One of the CF_3 fluorines in KNTfAc was disordered over a symmetry operation, which necessitated the use of PART -1 instructions to successfully model.

Table 1: crystallographic data for all structures. All datasets were collected at 173.0(1) K.

Compound	[H][N(Tf)(Ac)]	[K][N(Tf)(Ac)]	[H][N(TFA)(Ms)]	[H][N(Ms)(Ac)]	[NMe_4][$CH(Tf)_2$]
Formula	$C_3H_4F_3NO_3S$	$C_6H_8F_6K_2N_2O_7S_2$	$C_3H_4F_3NO_3S$	$C_3H_7NO_3S$	$C_7H_{13}F_6NO_4S_2$
M/g mol^{-1}	191.13	476.46	191.13	137.16	353.30
Crystal system	monoclinic	orthorhombic	monoclinic	orthorhombic	monoclinic
Space group (No.)	$P\,2_1/c$ (14)	$Cmma$ (67)	$P\,2_1/c$ (14)	$P\,2_12_12_1$	$P\,2_1/c$ (14)
a/Å	8.0868(5)	8.4456(7)	8.9112(10)	8.0559(2)	27.9524(7)
b/Å	9.2975(5)	21.7761(16)	5.0072(5)	8.4221(3)	10.6367(4)
c/Å	9.6955(6)	9.0436(5)	15.368(2)	9.1633(4)	19.2552(5)
α/°	90	90	90	90	90
β/°	95.255(5)	90	95.041(11)	90	90.426(2)
γ/°	90	90	90	90	90
U/Å^3	725.91(7)	1662.5(2)	683.07(14)	621.71(4)	5724.8(3)
Z	4	4	4	4	16
μ(Mo-Kα) /mm^{-1}	0.463	0.918	1.859	0.443	0.450
F(000)	384	952	384	288	2880
Total reflections	3103	4540	2083	4494	20502
Unique reflections	1819	1012	2083	1620	11490
R_{int}	0.023	0.019	0.035	0.024	0.027
GooF on F^2	1.072	1.085	0.980	1.102	1.047
R_1[b] [$I_o > 2\sigma(I_o)$]	0.042	0.028	0.036	0.030	0.072
R_1 (all data)	0.058	0.034	0.049	0.032	0.103
wR_2[b] [$I_o > 2\sigma(I_o)$]	0.088	0.071	0.077	0.071	0.164
wR_2 (all data)	0.097	0.075	0.080	0.072	0.185

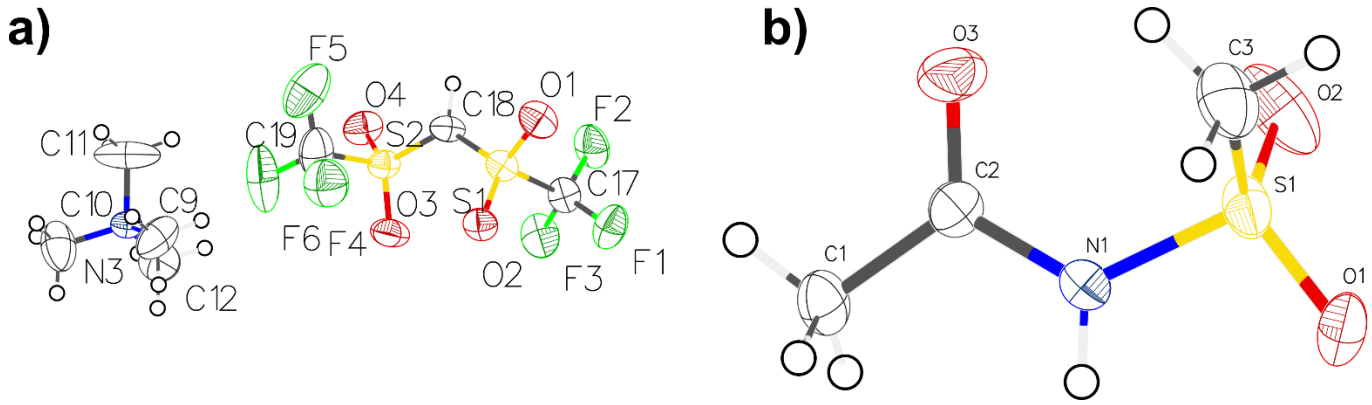

Figure 1: ORTEP plots of the additional crystal structures of a) [NMe_4][$CH(Tf)_2$] and b) [H][N(Ms)(Ac)]. Thermal ellipsoids at 50% probability.

The dihedral angles were read from the crystal structures for comparison with the dihedral angles obtained from the calculation, Table 2.

Table 2: Dihedral angles obtained from experimental and theoretical geometries.

Crystal structure geometry			Computational geometry		
	φ^1 / °	φ^2 / °	model	φ^1 / °	φ^2 / °
[H][N(Tf)(Ac)]	84	169	$[N(Tf)(Ac)]^-$	58	169
[H][N(Tf)(Ac)]	84	169	[H][N(Tf)(Ac)]	78	171
[K][N(Tf)(Ac)]	180	180	$[N(Tf)(Ac)]^-$	180	180
[H][N(TFA)(Ms)]	181	61	$[N(TFA)(Ms)]^-$	179	50
[H][N(TFA)(Ms)]	181	61	[H][N(TFA)(Ms)]	171	61
[H][N(Ms(Ac)]	58	179	$[N(Ms)(Ac)]^-$	51	174
[H][N(Ms)(Ac)]	58	179	[H][N(Ms)(Ac)]	64	164
[NMe_4][$CH(Tf)_2$]	95	89	$[CH(Tf)_2]^-$	87	87
[NMe_4][$CH(Tf)_2$]	94	88	$[CH(Tf)_2]^-$	87	87
[NMe_4][$CH(Tf)_2$]	92	89	$[CH(Tf)_2]^-$	87	87

Comparing all structures, a root-mean-square deviation (RMSD) of 8° is found. If only structures with matching model geometries are compared (i.e. not comparing crystal structures of the acid with computational geometries of anions and vice versa), then a root-mean-square deviation of 6° is found. The root-mean-square deviation decreases further to 4° if the crystal structures of the free acids are omitted.

3. Rheology

Experimental viscosities of the two ionic liquids [C_4C_1Im][N(Tf)(Ac)] and [C_4C_1Im][N(Ms)(TFA)], given in Table 3, were fitted with to the commonly used Vogel-Fulcher-Tammann (VFT) equation (1).[1–5]

$$\eta = \eta_0 \exp\left(\frac{B}{T - T_0}\right) \quad (1)$$

With the fit parameters reported in Table 4, a RMSD of 0.090 mPa s between experimental viscosities and viscosities predicted by the VFT equation is obtained.

Table 3: Experimental viscosities of the ionic liquids in this work.

	Viscosity / mPa s	
T / °C	[C_4C_1Im][N(Tf)(Ac)]	[C_4C_1Im][N(Ms)(TFA)]
25	149.39	292.47
30	111.98	204.89
35	85.36	147.98
40	67.09	110.38
45	53.29	84.02
50	43.10	65.45
55	35.45	52.04
60	29.50	42.06
65	24.84	34.40
70	21.13	28.61
75	18.20	24.16
80	15.83	20.62
85	13.84	17.79
90	12.23	15.44
95	10.87	13.57
100	9.74	11.98
105	8.73	10.65

Table 4: Fit parameters of the viscosity data to the VFT equation (1)

	η_0 / mPa s	$\Delta\eta_0$ / mPas	B / K	ΔB / K	T_0 / K	ΔT_0	R^2
[C_4C_1Im][N(Tf)(Ac)]	0.15516	0.00567	778.09	9.55	184.895	0.795	0.99999
[C_4C_1Im][N(Ms)(TFA)]	0.17016	0.00336	740.91	4.50	198.693	0.344	1.00000

4. Benchmark

4.1 Energy

Benchmark of different levels of theory for the energies of the five stationary points of the $[N(Tf)_2]^-$ anion, Table 5.

Table 5: Benchmark of different levels of theory for the energies of the five stationary points of the $[N(Tf)_2]^-$ anion.

	Stationary Points		Barriers		RMSD Barriers / kJ/mol	RMSD cis-trans / kJ/mol
	Name	Energy / kJ/mol	Name	Energy / kJ/mol		
MP2/6-311+G(d,p)	cis	3.78	cis to trans	5.04	0.89	0.24
	trans	0.00	trans to cis	8.82		
	TS1	8.82	cis to trans (higher)	21.53		
	TS2	11.42	trans to cis (higher)	25.31		
	TS3	25.31	cis to cis	7.64		
MP2/cc-pVDZ	cis	3.54	cis to trans	4.12	3.71	0.01
	trans	0.00	trans to cis	7.67		
	TS1	7.67	cis to trans (higher)	26.99		
	TS2	12.47	trans to cis (higher)	30.53		
	TS3	30.53	cis to cis	8.93		
MP2/aug-cc-pVDZ	cis	3.89	cis to trans	4.52	2.15	0.35
	trans	0.00	trans to cis	8.41		
	TS1	8.41	cis to trans (higher)	24.31		
	TS2	10.97	trans to cis (higher)	28.20		
	TS3	28.20	cis to cis	7.09		
MP2/cc-pVTZ	cis	3.65	cis to trans	3.78	0.31	0.11
	trans	0.00	trans to cis	7.43		
	TS1	7.43	cis to trans (higher)	21.58		
	TS2	10.82	trans to cis (higher)	25.23		
	TS3	25.23	cis to cis	7.17		
MP2=full/cc-pVTZ	cis	3.54	cis to trans	3.83	0.00	0.00
	trans	0.00	trans to cis	7.37		
	TS1	7.37	cis to trans (higher)	21.22		
	TS2	11.03	trans to cis (higher)	24.75		
	TS3	24.75	cis to cis	7.49		
M052X/6-311+G(d,p)	cis	2.28	cis to trans	4.70	1.58	1.25
	trans	0.00	trans to cis	6.98		
	TS1	6.98	cis to trans (higher)	19.59		
	TS2	10.58	trans to cis (higher)	21.87		
	TS3	21.87	cis to cis	8.30		
M06/6-311+G(d,p)	cis	2.49	cis to trans	4.78	1.80	1.04
	trans	0.00	trans to cis	7.27		
	TS1	7.27	cis to trans (higher)	19.24		
	TS2	11.53	trans to cis (higher)	21.74		
	TS3	21.74	cis to cis	9.03		
RB3LYP-GD3BJ/6-311+G(d,p)	cis	3.26	cis to trans	3.60	1.97	0.28
	trans	0.00	trans to cis	6.85		
	TS1	6.85	cis to trans (higher)	18.33		

	TS2	9.92	trans to cis (higher)	21.58		
	TS3	21.58	cis to cis	6.67		
ωB97XD/6-311+G(d,p)	cis	2.68	cis to trans	3.73	1.98	0.86
	trans	0.00	trans to cis	6.41		
	TS1	6.41	cis to trans (higher)	18.64		
	TS2	9.71	trans to cis (higher)	21.32		
	TS3	21.32	cis to cis	7.04		
B2PLYPD3/6-311+G(d,p)	cis	3.39	cis to trans	4.04	0.94	0.15
	trans	0.00	trans to cis	7.43		
	TS1	7.43	cis to trans (higher)	19.88		
	TS2	10.29	trans to cis (higher)	23.26		
	TS3	23.26	cis to cis	6.91		
B2PLYP/6-311+G(d,p)	cis	3.57	cis to trans	3.02	1.03	0.03
	trans	0.00	trans to cis	6.59		
	TS1	6.59	cis to trans (higher)	20.09		
	TS2	9.82	trans to cis (higher)	23.66		
	TS3	23.66	cis to cis	6.25		
B3LYP/6-311+G(d,p)	cis	3.15	cis to trans	2.10	2.02	0.39
	trans	0.00	trans to cis	5.25		
	TS1	5.25	cis to trans (higher)	19.14		
	TS2	9.06	trans to cis (higher)	22.29		
	TS3	22.29	cis to cis	5.91		
MP2/cc-pvtz// RB3LYP-GD3BJ/6-311+G(d,p)	cis	3.63	cis to trans	3.70	0.19	0.09
	trans	0.00	trans to cis	7.33		
	TS1	7.33	cis to trans (higher)	21.21		
	TS2	10.74	trans to cis (higher)	24.84		
	TS3	24.84	cis to cis	7.11		
MP2/cc-pvtz// M06 (reduced conv. crit)	cis	3.49	cis to trans	3.63	0.16	0.05
	trans	0.00	trans to cis	7.12		
	TS1	7.12	cis to trans (higher)	21.20		
	TS2	10.82	trans to cis (higher)	24.69		
	TS3	24.69	cis to cis	7.34		
MP2/cc-pvtz// M06/6-311+G(d,p)	cis	3.49	cis to trans	3.63	0.16	0.05
	trans	0.00	trans to cis	7.12		
	TS1	7.12	cis to trans (higher)	21.20		
	TS2	10.82	trans to cis (higher)	24.69		
	TS3	24.69	cis to cis	7.34		
B3LYP-GD3BJ/6-311+G(d,p) with SMD	cis	3.52	cis to trans	4.46	1.21	0.02
	trans	0.00	trans to cis	7.98		
	TS1	7.98	cis to trans (higher)	20.98		
	TS2	8.48	trans to cis (higher)	24.50		
	TS3	24.50	cis to cis	4.96		
M06-GD3/6-311+G(d,p)	cis	2.21	cis to trans	5.18	1.93	1.33
	trans	0.00	trans to cis	7.39		
	TS1	7.39	cis to trans (higher)	19.26		
	TS2	11.15	trans to cis (higher)	21.47		
	TS3	21.47	cis to cis	8.94		
HF/6-311+G(d,p)	cis	1.64	cis to trans	2.77	1.84	1.90

	trans	0.00	trans to cis	4.41		
	TS1	4.41	cis to trans (higher)	23.63		
	TS2	10.13	trans to cis (higher)	25.27		
	TS3	25.27	cis to cis	8.49		
M06/aug-cc-pVTZ	cis	2.42	cis to trans	4.27	2.32	1.12
	trans	0.00	trans to cis	6.69		
	TS1	6.69	cis to trans (higher)	18.21		
	TS2	10.31	trans to cis (higher)	20.63		
	TS3	20.63	cis to cis	7.89		
M06/aug-cc-pVDZ	cis	3.35	cis to trans	4.55	0.70	0.18
	trans	0.00	trans to cis	7.90		
	TS1	7.90	cis to trans (higher)	21.48		
	TS2	12.11	trans to cis (higher)	24.83		
	TS3	24.83	cis to cis	8.76		
MP2/cc-pvtz// M06/aug-cc-pVTZ	cis	3.35	cis to trans	3.75	0.19	0.18
	trans	0.00	trans to cis	7.10		
	TS1	7.10	cis to trans (higher)	21.30		
	TS2	10.55	trans to cis (higher)	24.65		
	TS3	24.65	cis to cis	7.19		
B3LYP-GD3BJ/6-311G(d,p)	cis	3.26	cis to trans	5.04	1.08	0.28
	trans	0.00	trans to cis	8.29		
	TS1	8.29	cis to trans (higher)	20.03		
	TS2	10.72	trans to cis (higher)	23.28		
	TS3	23.28	cis to cis	7.47		
B3LYP-GD3BJ/6-31+G(d,p)	cis	3.51	cis to trans	3.54	1.30	0.02
	trans	0.00	trans to cis	7.05		
	TS1	7.05	cis to trans (higher)	19.39		
	TS2	9.77	trans to cis (higher)	22.90		
	TS3	22.90	cis to cis	6.26		
MP2=full/cc-pVTZ// B3LYP-GD3BJ/6-311+G(d,p)	cis	3.47	cis to trans	3.66	0.28	0.07
	trans	0.00	trans to cis	7.13		
	TS1	7.13	cis to trans (higher)	20.88		
	TS2	10.81	trans to cis (higher)	24.35		
	TS3	24.35	cis to cis	7.34		
CCSD/cc-pVDZ	cis	3.48				0.06
	trans	0.00				
CCSD/cc-pvtz// CCSD/cc-pVDZ	cis	3.44				0.09
	trans	0.00				
CCSD(T)/cc-pVTZ// CCSD/cc-pVDZ	cis	3.44				0.09
	trans	0.00				
CCSD(T)/cc-pVDZ// CCSD/cc-pVDZ	cis	3.48				0.06
	trans	0.00				

4.2 Geometry

Benchmark of different levels of theory for the geometries of the five stationary points of the $[N(Tf)_2]^-$ anion, Table 6.

Table 6: Benchmark of different levels of theory for the geometries (backbone dihedral angles) of the five stationary points of the $[N(Tf)_2]^-$ anion.

	Name	φ^1 / °	Φ^2 / °	RMSD / °
MP2/6-311+G(d,p)	cis	83.3	-126.1	2.99
	trans	93.3	93.3	
	TS1	92.7	159.4	
	TS2	112.2	-112.3	
	TS3	99	-4.4	
MP2/cc-pVDZ	cis	85.4	-127.2	3.01
	trans	91.2	91.2	
	TS1	85.8	150.5	
	TS2	113.3	-113.3	
	TS3	97.1	-3.9	
MP2/aug-cc-pVDZ	cis	82.8	-123.5	4.02
	trans	91.2	91.2	
	TS1	82.8	153.3	
	TS2	107.4	-107.4	
	TS3	99.1	-6.1	
MP2/cc-pVTZ	cis	85.9	-128.4	0.44
	trans	92.5	92.5	
	TS1	89.5	153.7	
	TS2	112.6	-112.6	
	TS3	102.4	-7.9	
MP2=full/cc-pVTZ	cis	85.9	-128.3	0.00
	trans	92.6	92.6	
	TS1	89.1	154.2	
	TS2	112.9	-112.9	
	TS3	103.3	-8.6	
M052X/6-311+G(d,p)	cis	84.1	-127.6	2.21
	trans	93	93	
	TS1	93.2	154.2	
	TS2	114.2	-114.2	
	TS3	100.1	-4.8	
M06/6-311+G(d,p)	cis	83.4	-128.3	1.68

	trans	93.3	93.3	
	TS1	92.5	155.3	
	TS2	114.8	-114.8	
	TS3	102.6	-9.4	
B3LYP-GD3BJ/6-311+G(d,p)	cis	84	-128.7	2.59
	trans	92.4	92.4	
	TS1	88.8	156	
	TS2	109	-109	
	TS3	99	-5.3	
ωB97XD/6-311+G(d,p)	cis	87.2	-134.5	2.70
	trans	94.1	94.1	
	TS1	92.3	155.8	
	TS2	111.5	-111.5	
	TS3	101.4	-5.8	
B2PLYPD3/6-311+G(d,p)	cis	83.6	-127.1	2.65
	trans	92.6	92.6	
	TS1	90.5	157.2	
	TS2	110.3	-110.3	
	TS3	98.5	-4.6	
B2PLYP/6-311+G(d,p)	cis	85.7	-130.8	2.68
	trans	93.4	93.4	
	TS1	92.1	155.9	
	TS2	111.4	-111.4	
	TS3	98.4	-3.7	
B3LYP/6-311+G(d,p)	cis	93.7	-155.1	9.16
	trans	94.1	94.1	
	TS1	92.7	152.9	
	TS2	111.5	-111.5	
	TS3	99.5	-3.9	
B3LYP-GD3BJ/6-311+G(d,p) with SMD	cis	83.4	-121	6.15
	trans	91.5	91.5	
	TS1	86	155.6	
	TS2	100.4	-102.7	
	TS3	97.8	-4.8	
M06-GD3/6-311+G(d,p)	cis	83.4	-128.2	1.80
	trans	94.4	94.4	

	TS1	92.7	155.6	
	TS2	114.2	-114.2	
	TS3	102.7	-9.6	
HF/6-311+G(d,p)	cis	100.6	-169	14.86
	trans	95.2	95.2	
	TS1	98.3	144.3	
	TS2	120.4	-120.4	
	TS3	102.7	-3.4	
M06/aug-cc-pVTZ	cis	84.3	-128.6	1.82
	trans	94.3	94.3	
	TS1	89.5	153.6	
	TS2	114.2	-114.5	
	TS3	105.5	-12.5	
M06/aug-cc-pVDZ	cis	82.3	-126.8	2.11
	trans	93.7	93.7	
	TS1	84.2	154.1	
	TS2	112.7	-112.8	
	TS3	102	-9.6	
B3LYP-GD3BJ/6-311G(d,p)	cis	80.3	-122.1	4.91
	trans	90.5	90.5	
	TS1	85.3	155.1	
	TS2	106.1	-106.1	
	TS3	97.3	-4.3	
B3LYP-GD3BJ/6-31+G(d,p)	cis	83	-127	3.42
	trans	91.2	91.2	
	TS1	87.8	150.7	
	TS2	107.2	-107.2	
	TS3	99.1	-6.1	
CCSD/cc-pVDZ	cis	85.4	-129.4	1.22
	trans	91.1	91.1	

5. Additional molecular orbitals

For $O(Tf)_2$ and $[CH(Tf)_2]^-$, HOMO-8 and HOMO-18 directly correspond to the respective molecular orbitals in $[N(Tf)_2]^-$, Figure 2.

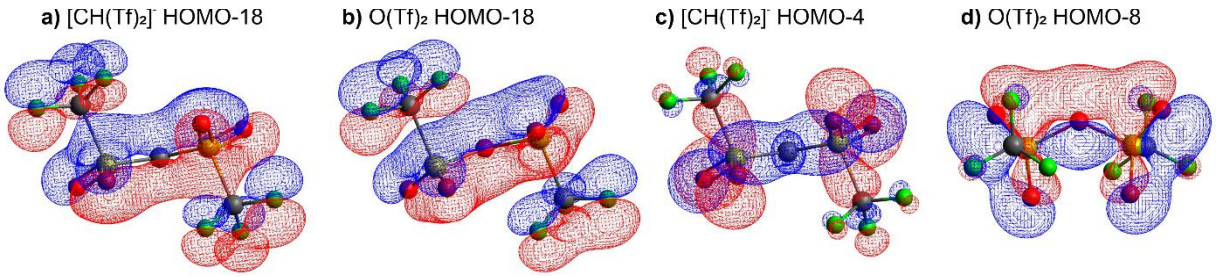

Figure 2: Molecular orbitals showing the delocalisation in $[CH(Tf)_2]^-$ and $O(Tf)_2$.

6. Key structures

The $[N(Tf)(TFA)]^-$ anion shows a flat structure as global minimum, from which other minima are obtained by tilting one of the end groups out of the paper plane, Figure 3.

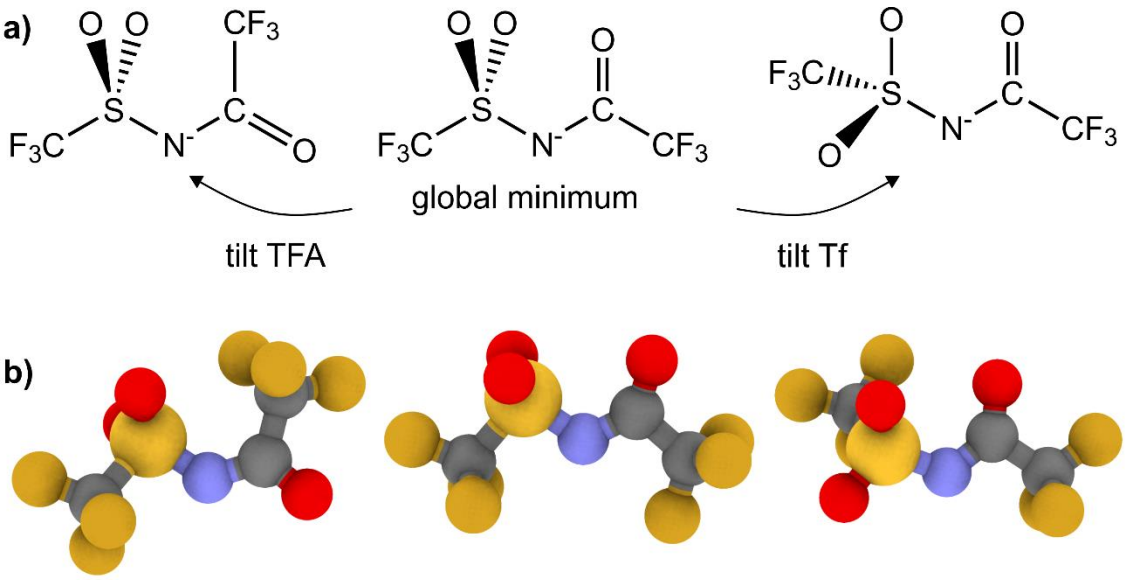

*Figure 3: minimum structures of $[N(Tf)(TFA)]^-$. **a)** schematic representation of the tilted groups, **b)** optimised minimum geometries.*

7. NBO charges

The delocalisation of negative charge over the fluorinated end groups in $[N(Tf)_2]^-$ is visible in the natural bond orbital analysis (NBO) charges of $[N(Tf)_2]^-$ in comparison with those of $[N(Ms)_2]^-$, Table 7.

Table 7: Sum of the NBO charges for the central group (nitrogen atom), the sulfur atoms, the oxygen atoms and the end groups (CH_3 for $[N(Ms)_2]^-$ and CF_3 for $[N(Tf)_2]^-$).

	$[N(Ms)_2]^-$	$[N(Tf)_2]^-$
Central group	-1.20	-1.19
Sulfur	4.36	4.26
Oxygen	-3.90	-3.64
End groups	-0.26	-0.42

8. Stationary points

Below are given the stationary points for charged (Table 8) and neutral (Table 9) analogues.

Table 8: Equilibrium dihedral angles of the backbone, type of the stationary point (GS = ground state local minimum, TS = transition state), and energy referenced to the global minimum for the negatively charged structures. Xyz files of all structures can be found in the folder 'anion_structures'.

system	type	φ^1 / °	φ^2 / °	kJ/mol	system	type	φ^1 / °	φ^2 / °	kJ/mol
$[CH(Ac)_2]^-$	GS	0	180	0.0	$[N(Sf)_2]^-$	GS	63	63	0.0
$[CH(Ac)_2]^-$	GS	0	0	20.9	$[N(Sf)_2]^-$	GS	50	215	18.0
$[CH(Ac)_2]^-$	GS	180	180	27.7	$[N(Sf)_2]^-$	TS	113	344	18.3
$[CH(Ac)_2]^-$	TS	89	184	90.3	$[N(Sf)_2]^-$	TS	62	298	27.2
$[CH(Ac)_2]^-$	TS	1	90	97.8	$[N(Sf)_2]^-$	TS	52	151	29.9
$[CH(Fs)_2]^-$	GS	75	285	0.0	$[N(Tf)_2]^-$	GS	92	92	0.0
$[CH(Fs)_2]^-$	GS	84	84	0.2	$[N(Tf)_2]^-$	GS	84	231	3.5
$[CH(Fs)_2]^-$	TS	79	199	27.3	$[N(Tf)_2]^-$	TS	89	156	7.1
$[CH(Fs)_2]^-$	TS	16	64	32.9	$[N(Tf)_2]^-$	TS	109	251	10.8
$[CH(Ms)_2]^-$	GS	65	76	0.0	$[N(Tf)_2]^-$	TS	99	355	24.3
$[CH(Ms)_2]^-$	GS	132	293	28.8	$[N(TFA)_2]^-$	TS	180	180	0.0
$[CH(Ms)_2]^-$	TS	73	287	29.3	$[N(TFA)_2]^-$	GS	163	163	0.4
$[CH(Ms)_2]^-$	TS	0	77	38.7	$[N(TFA)_2]^-$	GS	44	195	4.3
$[CH(Ms)_2]^-$	TS	61	209	43.5	$[N(TFA)_2]^-$	GS	43	43	13.5
$[CH(Tf)_2]^-$	GS	87	87	0.0	$[N(TFA)_2]^-$	TS	96	181	13.7
$[CH(Tf)_2]^-$	GS	101	273	7.5	$[N(TFA)_2]^-$	TS	4	93	20.1
$[CH(Tf)_2]^-$	TS	96	264	7.6	$[N(TFA)(Ac)]^-$	GS	191	34	0.0
$[CH(Tf)_2]^-$	TS	84	189	41.0	$[N(TFA)(Ac)]^-$	TS	180	0	1.8
$[CH(Tf)_2]^-$	TS	91	359	53.0	$[N(TFA)(Ac)]^-$	GS	167	146	13.0
$[CH(TFA)_2]^-$	GS	180	180	0.0	$[N(TFA)(Ac)]^-$	TS	180	180	14.1
$[CH(TFA)_2]^-$	GS	180	0	2.8	$[N(TFA)(Ac)]^-$	GS	40	205	16.5
$[CH(TFA)_2]^-$	GS	22	22	30.9	$[N(TFA)(Ac)]^-$	GS	32	46	22.6
$[CH(TFA)_2]^-$	TS	92	181	74.3	$[N(TFA)(Ac)]^-$	TS	5	88	27.3
$[CH(TFA)_2]^-$	TS	95	359	83.5	$[N(TFA)(Ac)]^-$	TS	0	180	29.3
$[CH(Tf)(TFA)]^-$	GS	78	179	0.0	$[N(TFA)(Ac)]^-$	TS	98	180	31.2
$[CH(Tf)(TFA)]^-$	GS	92	2	11.8	$[N(TFA)(Ac)]^-$	TS	88	6	33.0

$[CH(Tf)(TFA)]^-$	TS	180	180	28.4	$[N(Tf)(Ac)]^-$	GS	89	5	0.0
$[CH(Tf)(TFA)]^-$	TS	0	180	34.3	$[N(Tf)(Ac)]^-$	GS	187	0	0.3
$[CH(Tf)(TFA)]^-$	TS	180	0	41.7	$[N(Tf)(Ac)]^-$	TS	110	13	1.5
$[CH(Tf)(TFA)]^-$	TS	80	104	90.9	$[N(Tf)(Ac)]^-$	GS	180	180	1.7
$[N(Ac)_2]^-$	GS	29	193	0.0	$[N(Tf)(Ac)]^-$	GS	58	170	4.7
$[N(Ac)_2]^-$	GS	153	153	15.5	$[N(Tf)(Ac)]^-$	TS	108	190	9.0
$[N(Ac)_2]^-$	TS	173	109	20.0	$[N(Tf)(Ac)]^-$	TS	0	180	17.7
$[N(Ac)_2]^-$	GS	37	37	20.2	$[N(Tf)(Ac)]^-$	TS	81	99	19.9
$[N(Ac)_2]^-$	TS	5	87	27.5	$[N(Tf)(Ac)]^-$	TS	93	261	24.1
$[N(Fs)_2]^-$	GS	76	76	0.0	$[N(TFA)(Ms)]^-$	GS	179	50	0.0
$[N(Fs)_2]^-$	GS	65	270	4.3	$[N(TFA)(Ms)]^-$	GS	180	180	12.0
$[N(Fs)_2]^-$	TS	77	283	4.6	$[N(TFA)(Ms)]^-$	TS	185	113	22.5
$[N(Fs)_2]^-$	TS	72	157	13.0	$[N(TFA)(Ms)]^-$	GS	0	196	33.6
$[N(Fs)_2]^-$	TS	2	69	17.2	$[N(TFA)(Ms)]^-$	TS	8	107	40.7
$[N(Ms)_2]^-$	GS	72	72	0.0	$[N(TFA)(Ms)]^-$	TS	89	83	52.3
$[N(Ms)_2]^-$	GS	70	200	22.2	$[N(TFA)(Ms)]^-$	TS	87	267	56.8
$[N(Ms)_2]^-$	TS	48	159	27.4	$[N(TFA)(Ms)]^-$	TS	180	0	7.5
$[N(Ms)_2]^-$	TS	90	350	33.7	$[N(Tf)(TFA)]^-$	GS	180	180	0.0
$[N(Ms)_2]^-$	TS	82	278	39.1	$[N(Tf)(TFA)]^-$	GS	74	173	2.3
$[N(Ms)(Ac)]^-$	GS	51	174	0.0	$[N(Tf)(TFA)]^-$	TS	108	186	6.9
$[N(Ms)(Ac)]^-$	GS	180	0	8.5	$[N(Tf)(TFA)]^-$	TS	0	180	15.7
$[N(Ms)(Ac)]^-$	TS	0	180	8.6	$[N(Tf)(TFA)]^-$	GS	202	355	18.9
$[N(Ms)(Ac)]^-$	GS	180	180	15.1	$[N(Tf)(TFA)]^-$	TS	94	90	32.3
$[N(Ms)(Ac)]^-$	TS	116	182	27.1	$[N(Tf)(TFA)]^-$	TS	265	75	39.0
$[N(Ms)(Ac)]^-$	TS	74	91	33.6					
$[N(Ms)(Ac)]^-$	TS	95	261	53.2					

Table 9: Equilibrium dihedral angles of the backbone, type of the stationary point (GS = local minimum, TS = transition state), and energy referenced to the global minimum for the neutral structures. Xyz files of all structures can be found in the folder 'neutral_structures'.

system	type	φ^1 / °	φ^2 / °	kJ/mol	system	type	φ^1 / °	φ^2 / °	kJ/mol
$NH(Tf)_2$	GS	88	88	0.0	$O(Sf)_2$	GS	66	66	0.0
$NH(Tf)_2$	GS	121	271	7.4	$O(Sf)_2$	GS	58	211	11.8
$NH(Tf)_2$	TS	106	254	9.8	$O(Sf)_2$	TS	114	351	16.9
$NH(Tf)_2$	TS	84	193	33.9	$O(Sf)_2$	TS	65	150	21.9
$NH(Tf)_2$	TS	105	348	46.1	$O(Sf)_2$	TS	89	271	27.4
$O(Fs)_2$	GS	76	76	0.0	$O(Tf)_2$	GS	94	94	0.0
$O(Fs)_2$	GS	80	202	4.8	$O(Tf)_2$	GS	98	203	3.5
$O(Fs)_2$	GS	60	271	4.9	$O(Tf)_2$	TS	94	151	6.8
$O(Fs)_2$	TS	74	219	5.9	$O(Tf)_2$	TS	120	240	11.7
$O(Fs)_2$	TS	74	286	6.1	$O(Tf)_2$	TS	101	356	27.6
$O(Fs)_2$	TS	65	159	10.5	$NH(Fs)_2$	GS	81	81	0.0
$O(Fs)_2$	TS	5	62	16.3	$NH(Fs)_2$	GS	71	289	2.3
$O(Fs)_2$	TS	0	180	19.8	$NH(Fs)_2$	TS	76	207	18.6
$O(Ms)_2$	GS	75	75	0.0	$NH(Fs)_2$	TS	15	58	23.9
$O(Ms)_2$	GS	77	194	15.1	$NH(Ms)_2$	GS	68	78	0.0
$O(Ms)_2$	TS	58	166	19.0	$NH(Ms)_2$	GS	147	283	23.3
$O(Ms)_2$	TS	0	180	24.5	$NH(Ms)_2$	TS	92	268	33.7
$O(Ms)_2$	TS	97	263	37.9	$NH(Ms)_2$	TS	15	261	41.0

9. Potential energy surfaces

The energies of 2D scans in this work are given in the folder ‘scan_results’ as POSIX text files. In these files, the first column corresponds to the dihedral from the group which is mentioned first. E.g. in ‘MP2RESULTS_ENERGIES_NMsTFA’, the first column corresponds to the C-S-N-C dihedral angle from the methanesulfonyl group, and the second column corresponds to the C-C-N-S dihedral angle from the trifluoroacetyl group. The third column contains the respective energies, given in Hartree. All angles are given in degrees, using the 0-360° convention. Additionally, 2D plots of all scanned surfaces are shown below, Figure 4 to Figure 27. Legend: red crosses = transition states, black crosses = local minima, dashed line = 15 kJ/mol threshold, red pluses = dihedral angles from crystal structures.

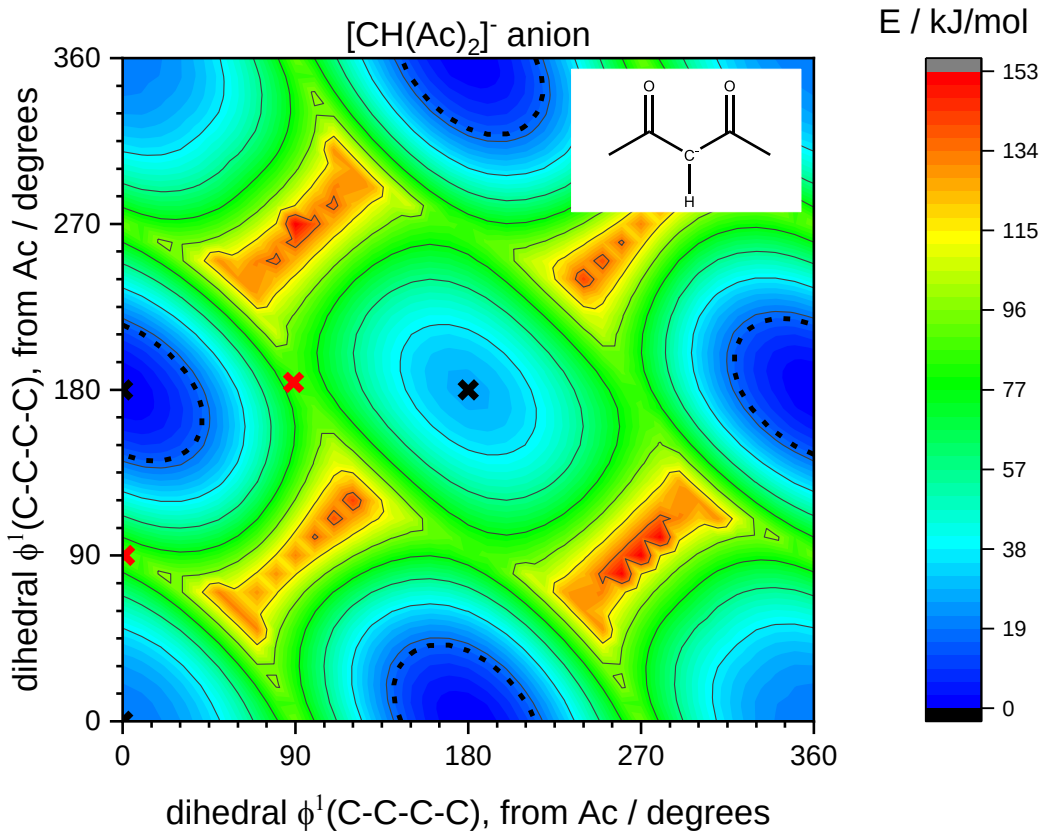

Figure 4: Potential Energy Surface of the $[CH(Ac)_2]^-$ anion.

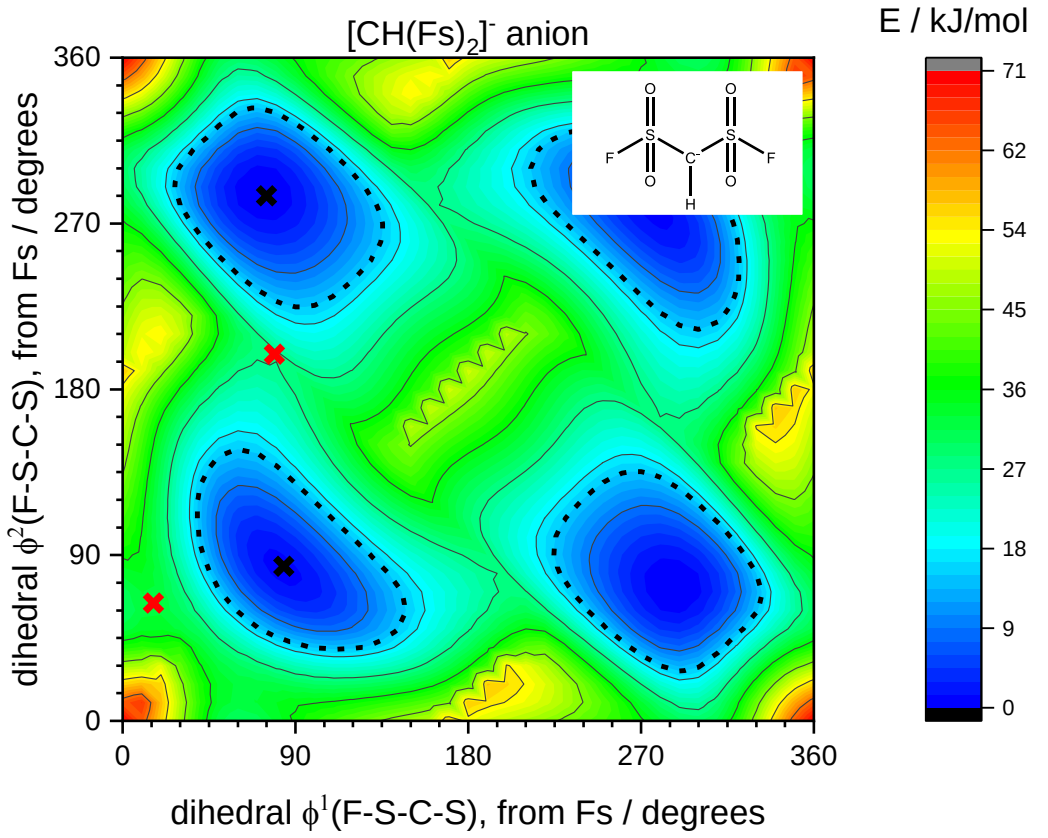

Figure 5: Potential Energy Surface of the $[CH(Fs)_2]^-$ anion.

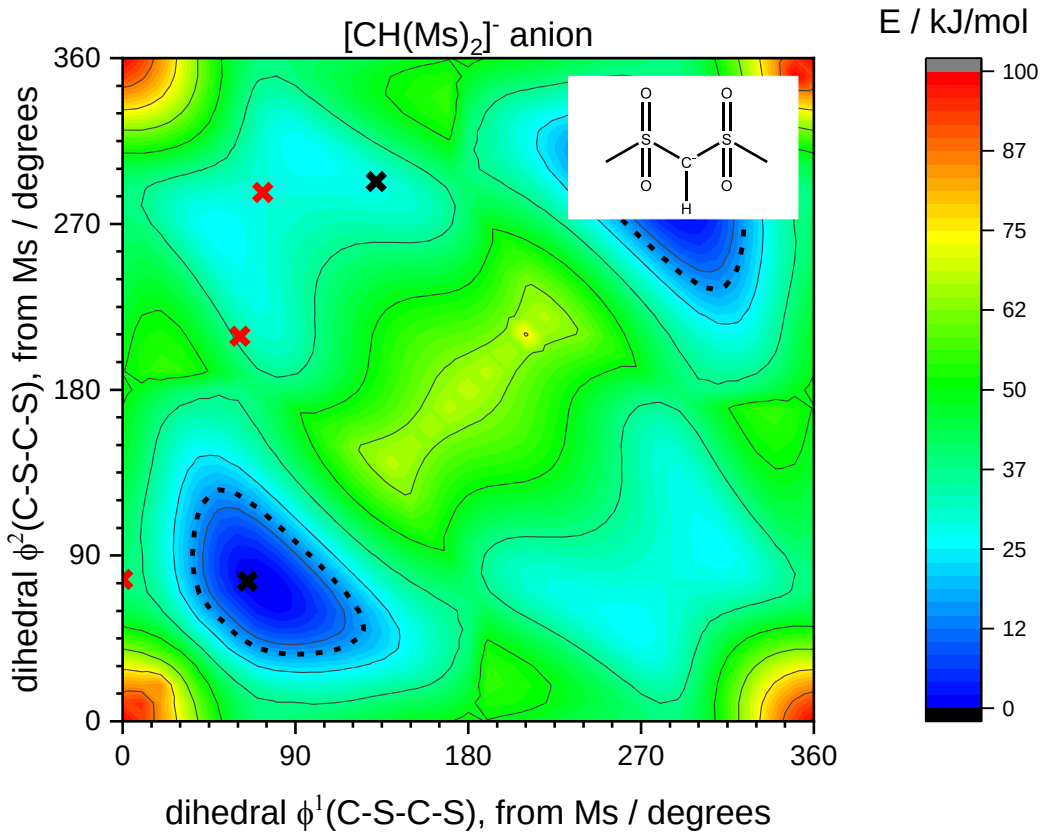

Figure 6: Potential Energy Surface of the $[CH(Ms)_2]^-$ anion.

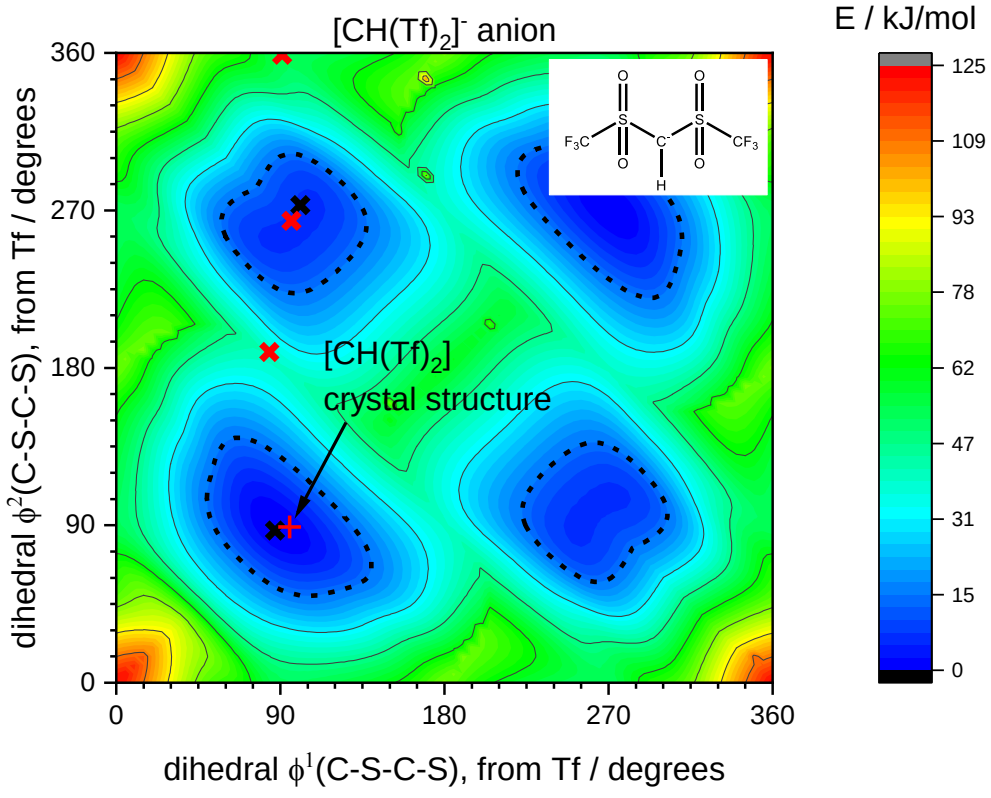

Figure 7: Potential Energy Surface of the $[CH(Tf)_2]^-$ anion.

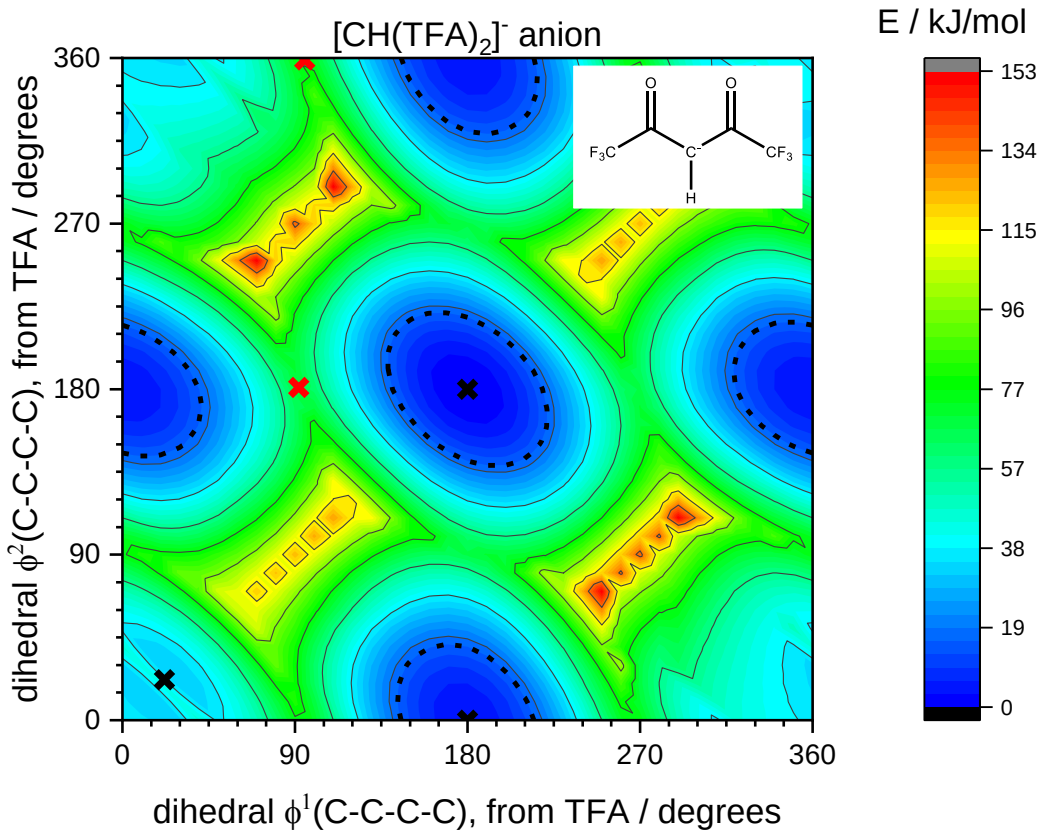

Figure 8: Potential Energy Surface of the $[CH(TFA)_2]^-$ anion.

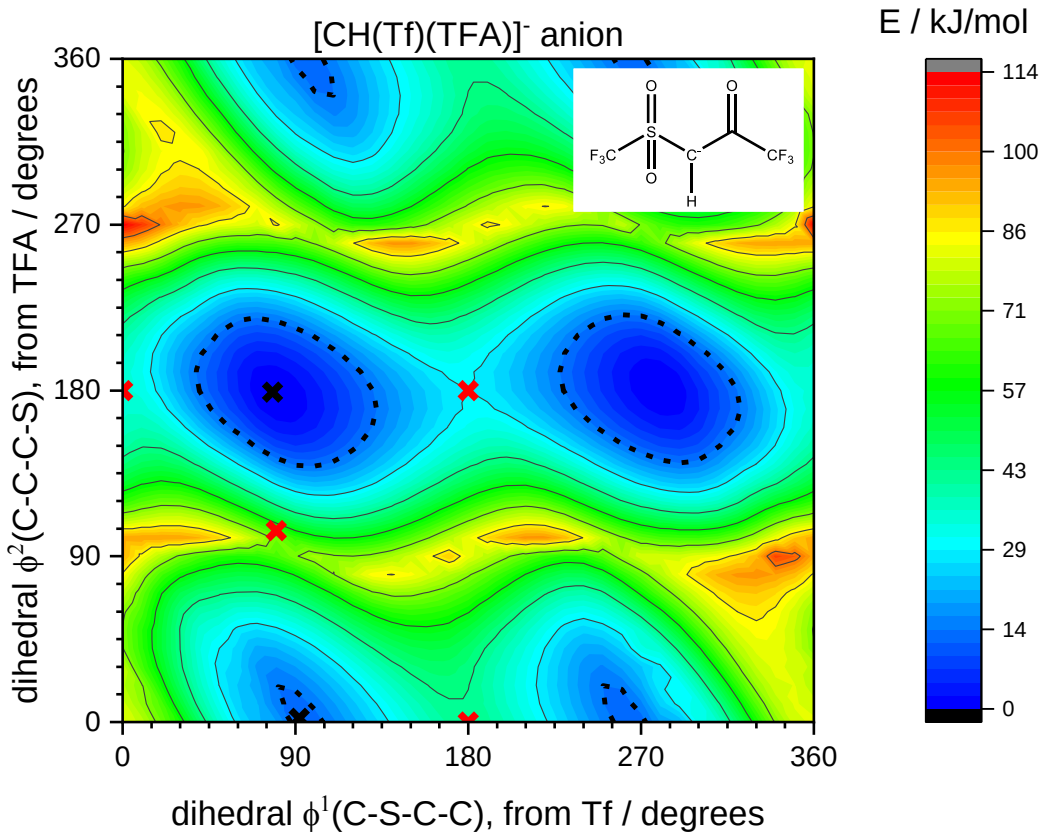

Figure 9: Potential Energy Surface of the $[CH(Tf)(TFA)]^-$ anion.

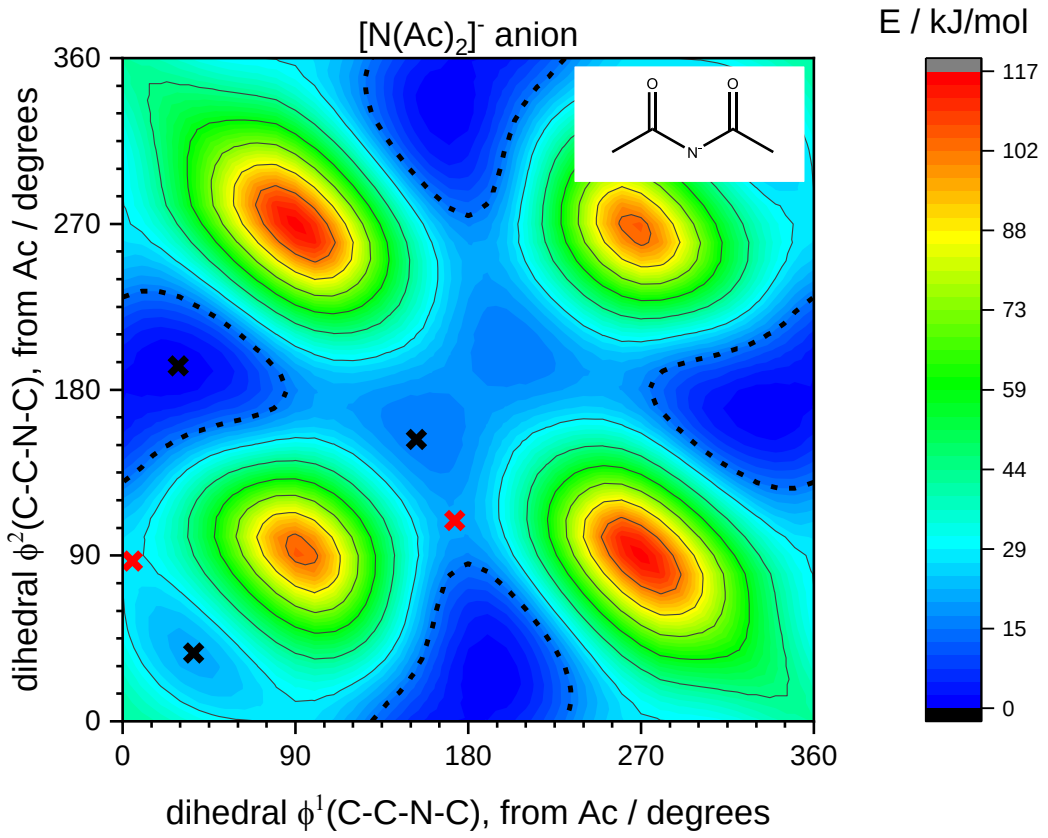

Figure 10: Potential Energy Surface of the $[N(Ac)_2]^-$ anion.

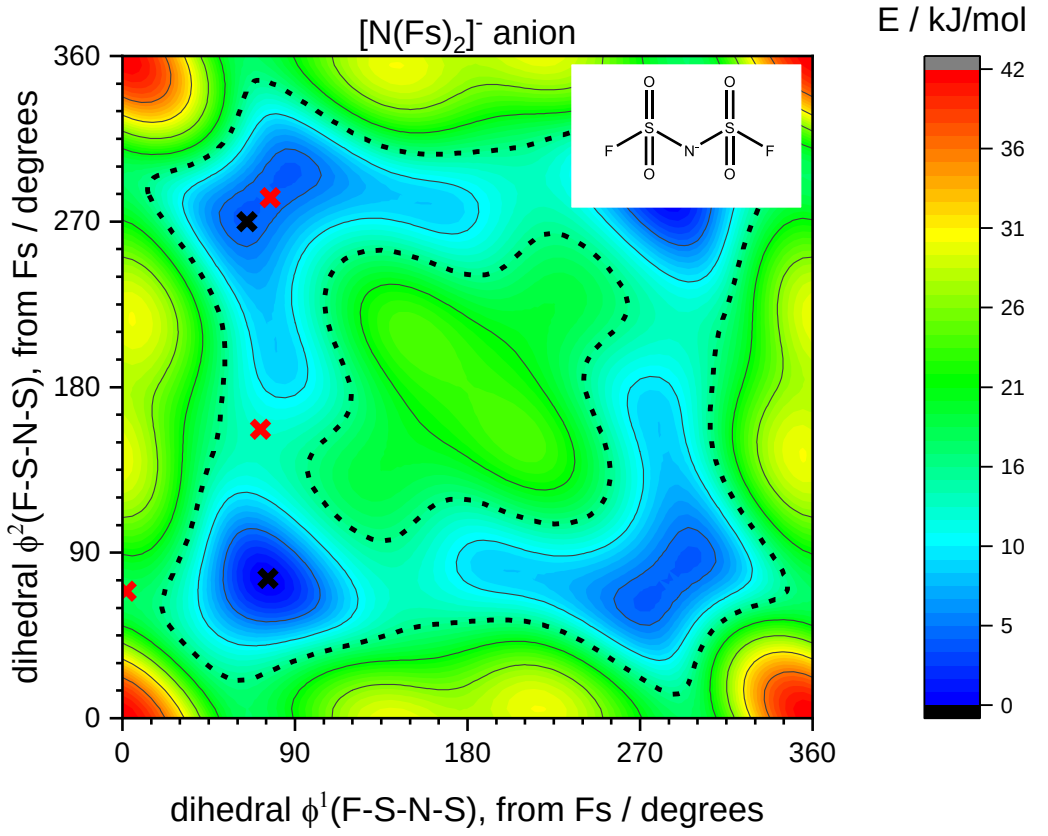

Figure 11: Potential Energy Surface of the $[N(Fs)_2]^-$ anion.

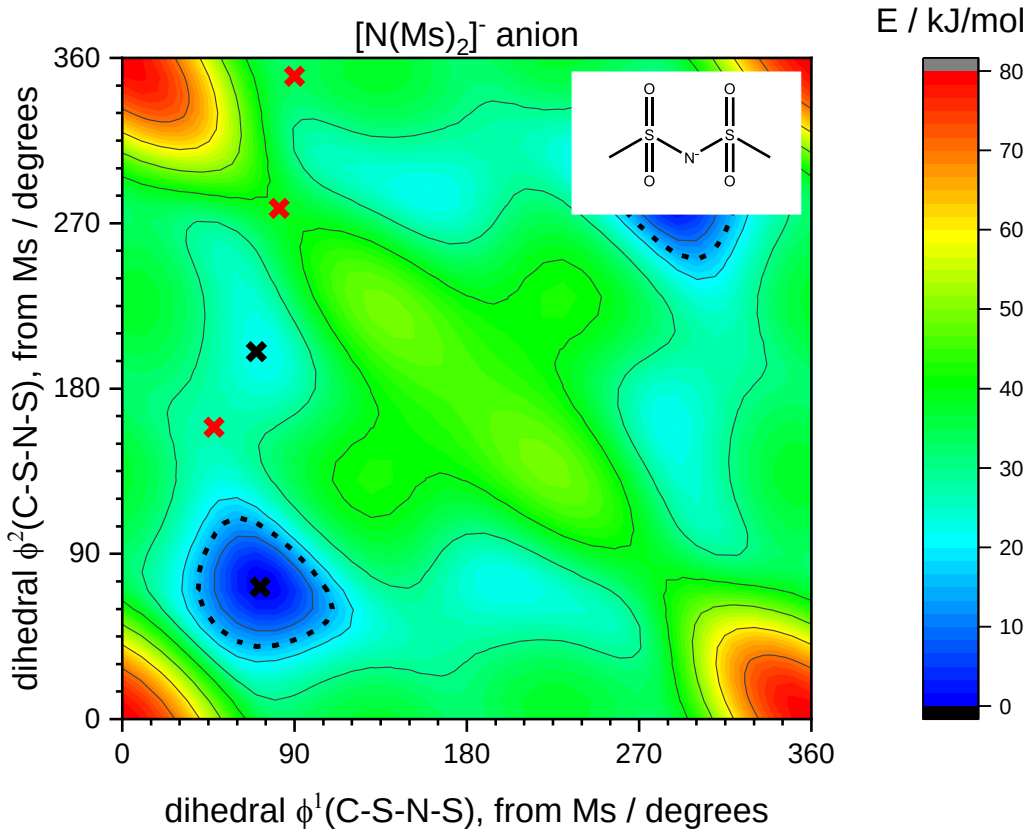

Figure 12: Potential Energy Surface of the $[N(Ms)_2]^-$ anion.

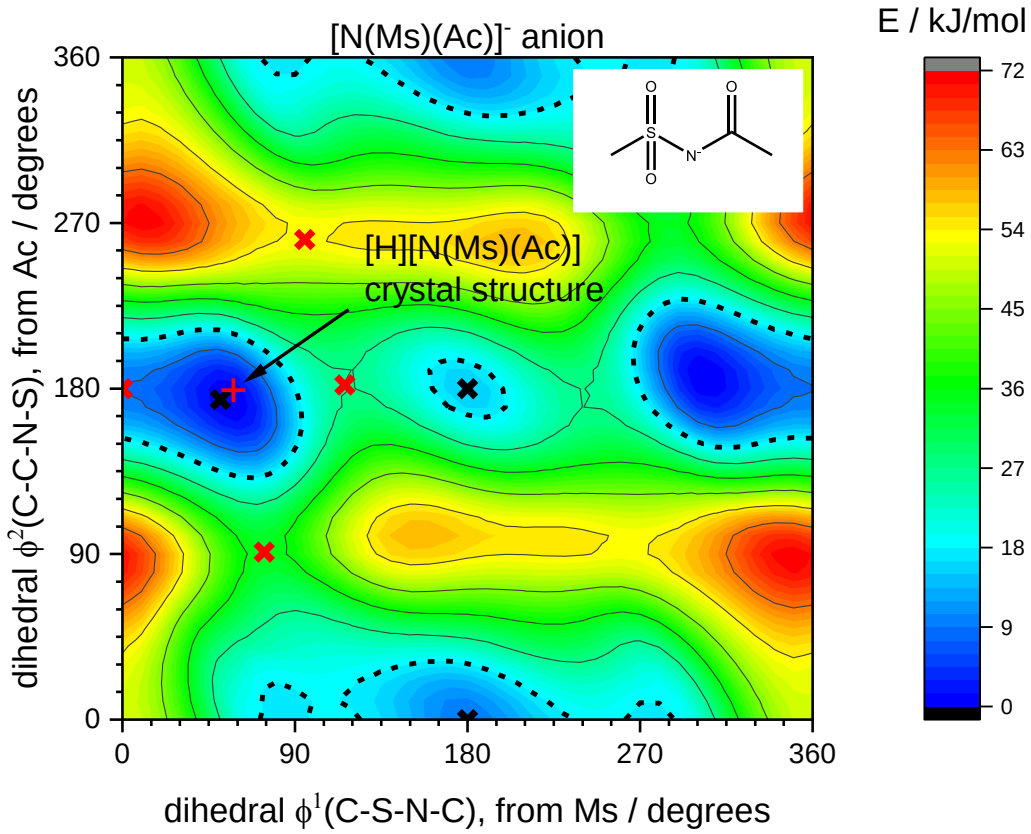

Figure 13: Potential Energy Surface of the $[N(Ms)(Ac)]^-$ anion.

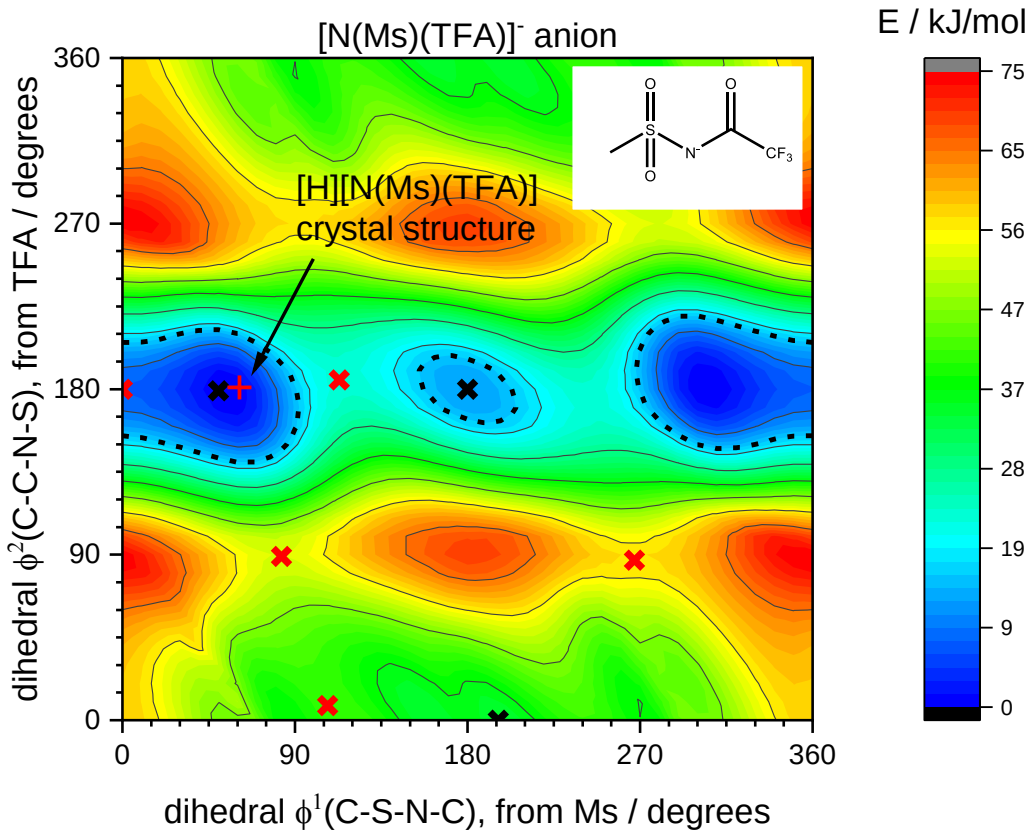

Figure 14: Potential Energy Surface of the [N(Ms)(TFA)]⁻ anion.

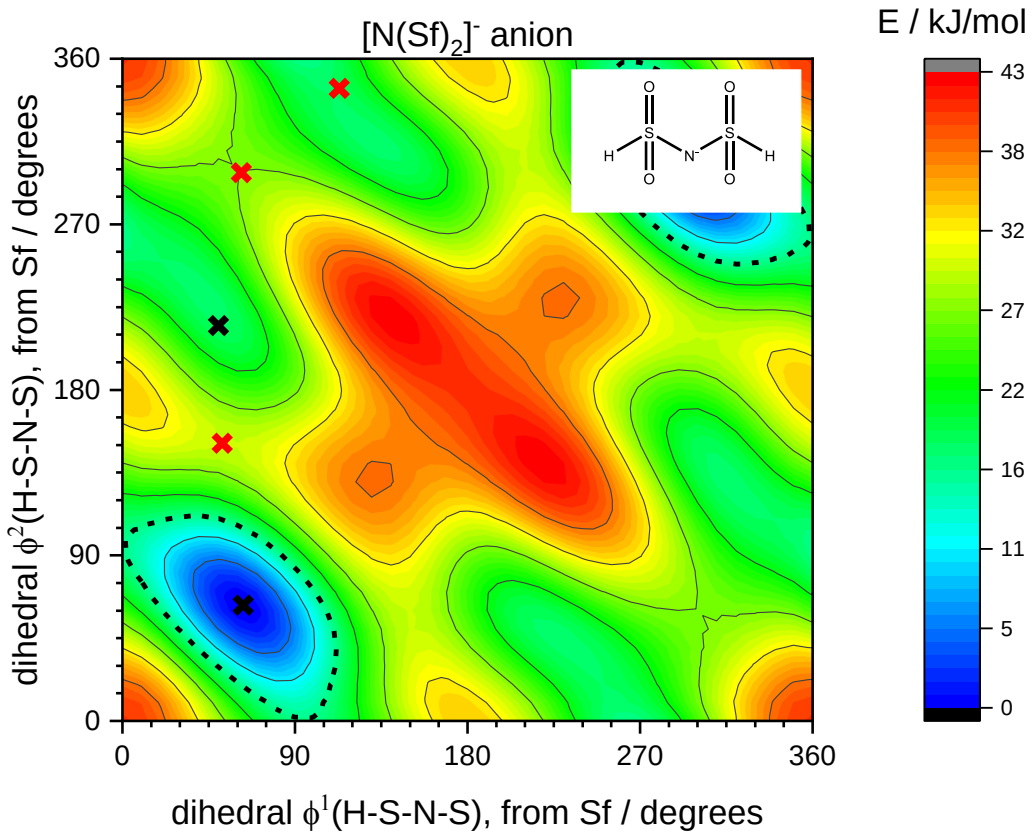

Figure 15: Potential Energy Surface of the [N(Sf)₂]⁻ anion.

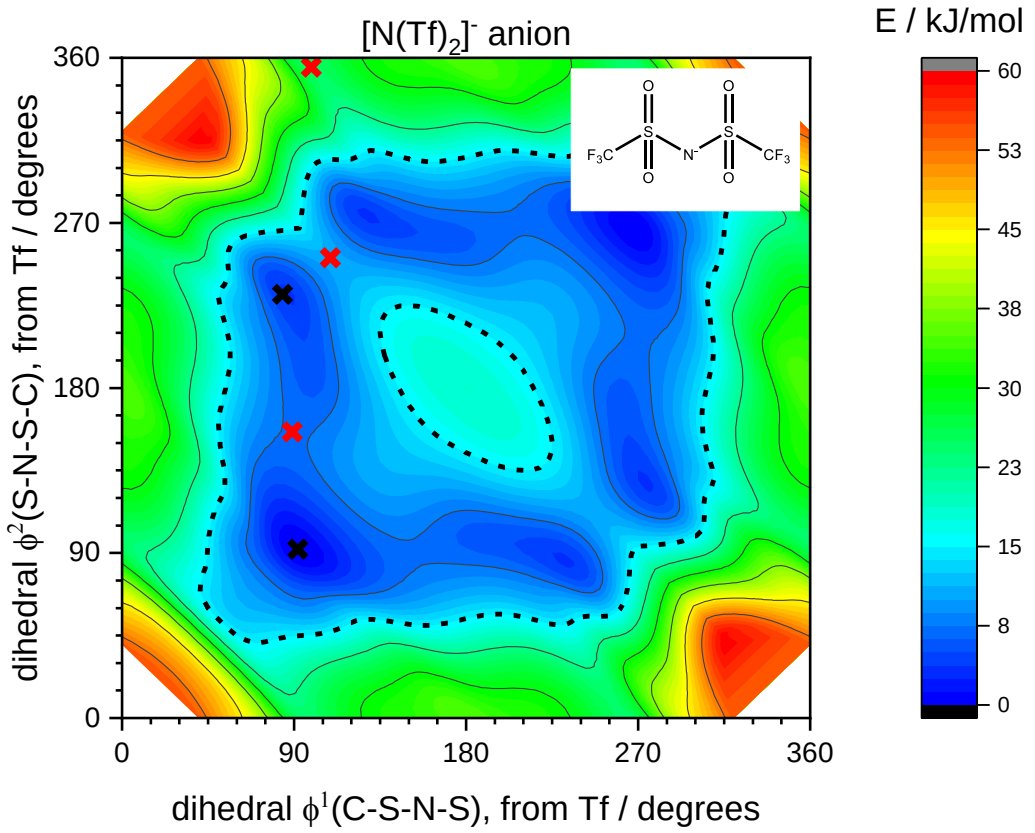

Figure 16: Potential Energy Surface of the $[N(Tf)_2]^-$ anion.

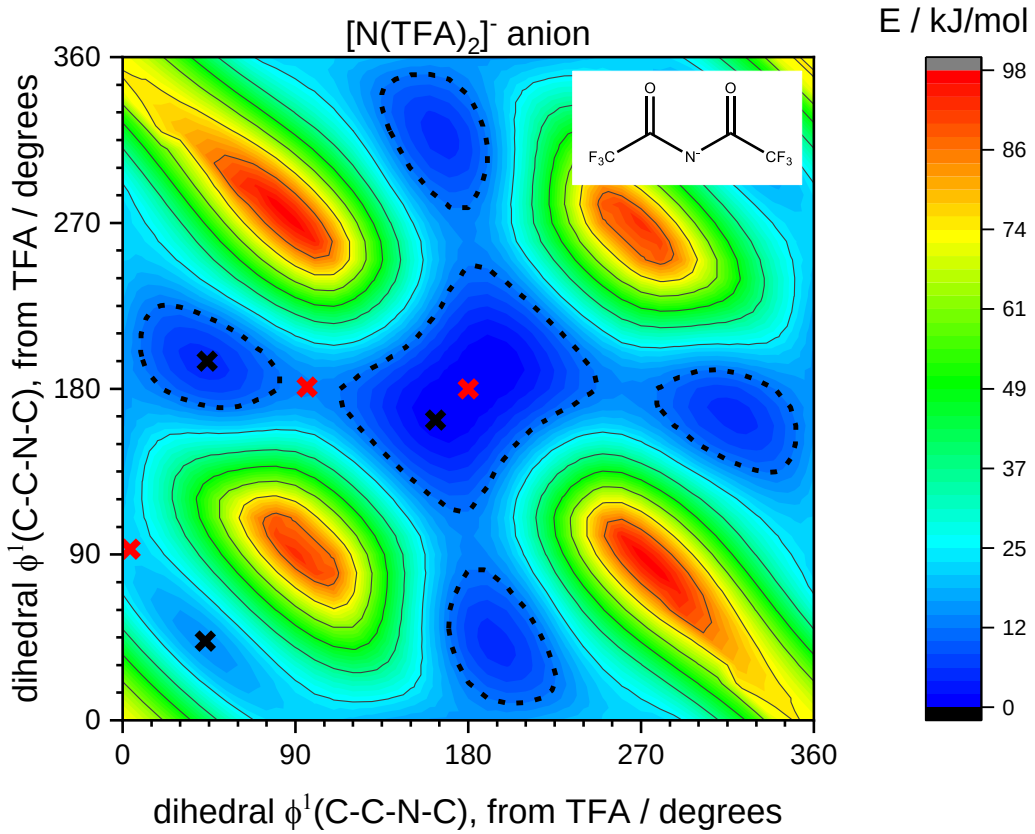

Figure 17: Potential Energy Surface of the $[N(TFA)_2]^-$ anion.

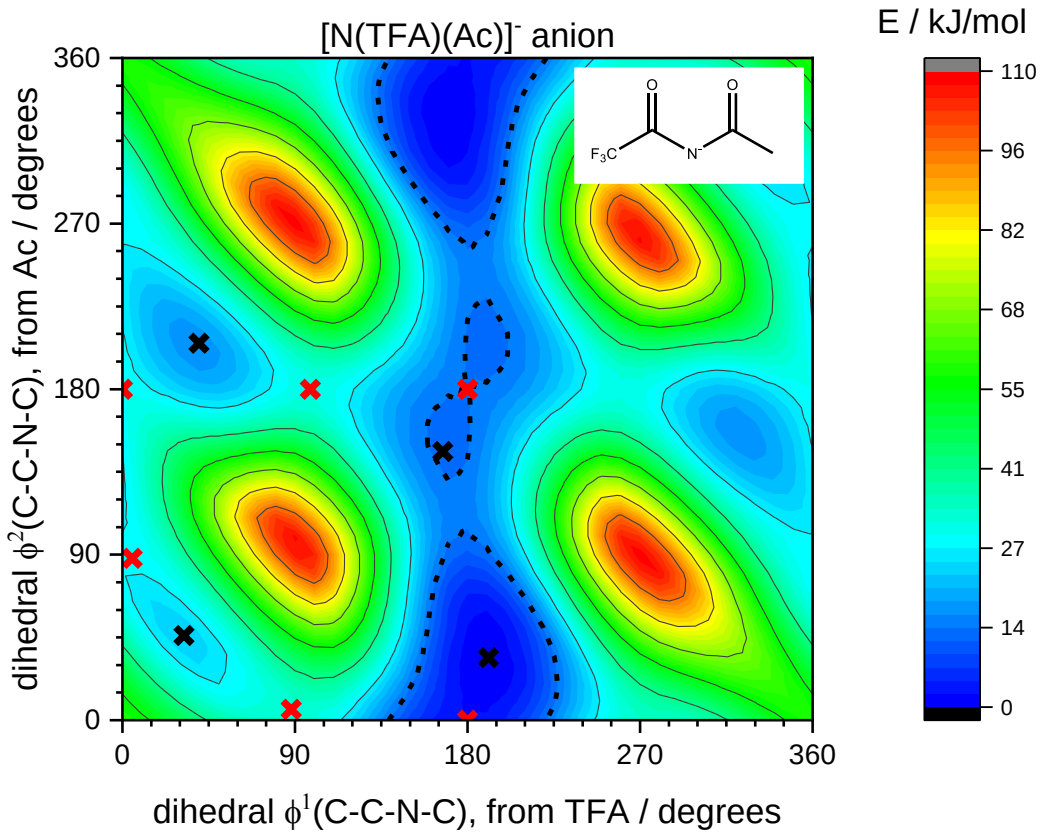

Figure 18: Potential Energy Surface of the [N(TFA)(Ac)]⁻ anion.

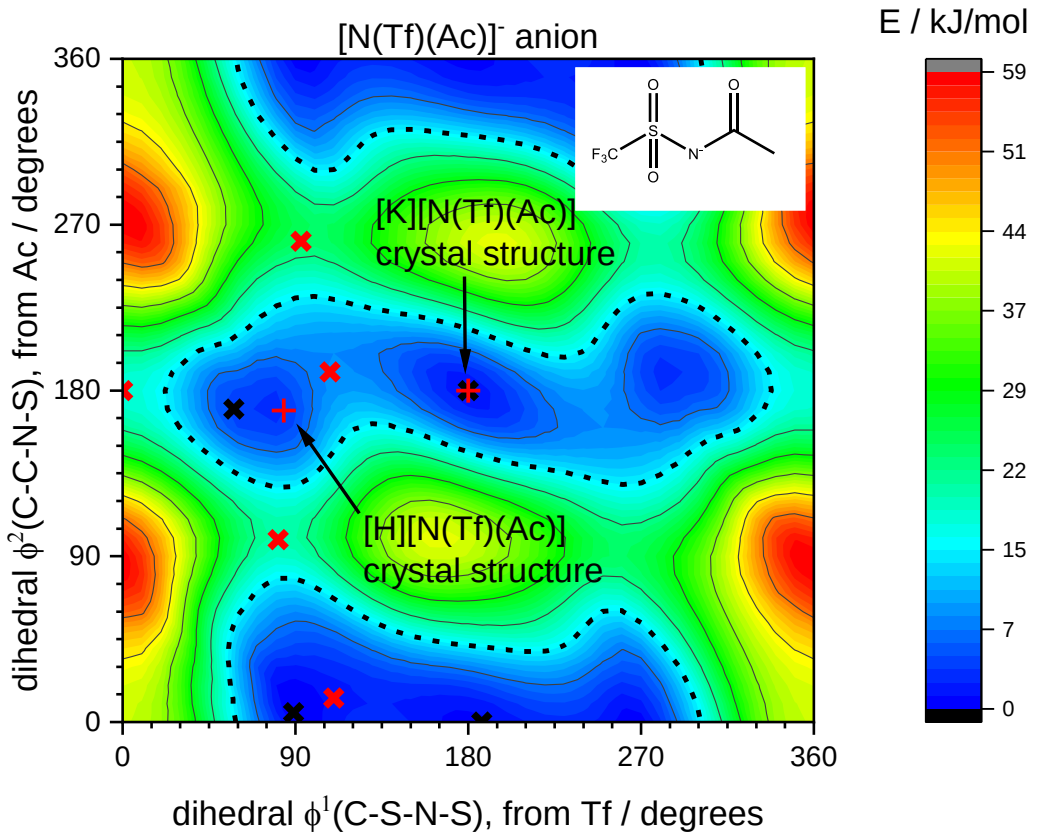

Figure 19: Potential Energy Surface of the [N(Tf)(Ac)]⁻ anion.

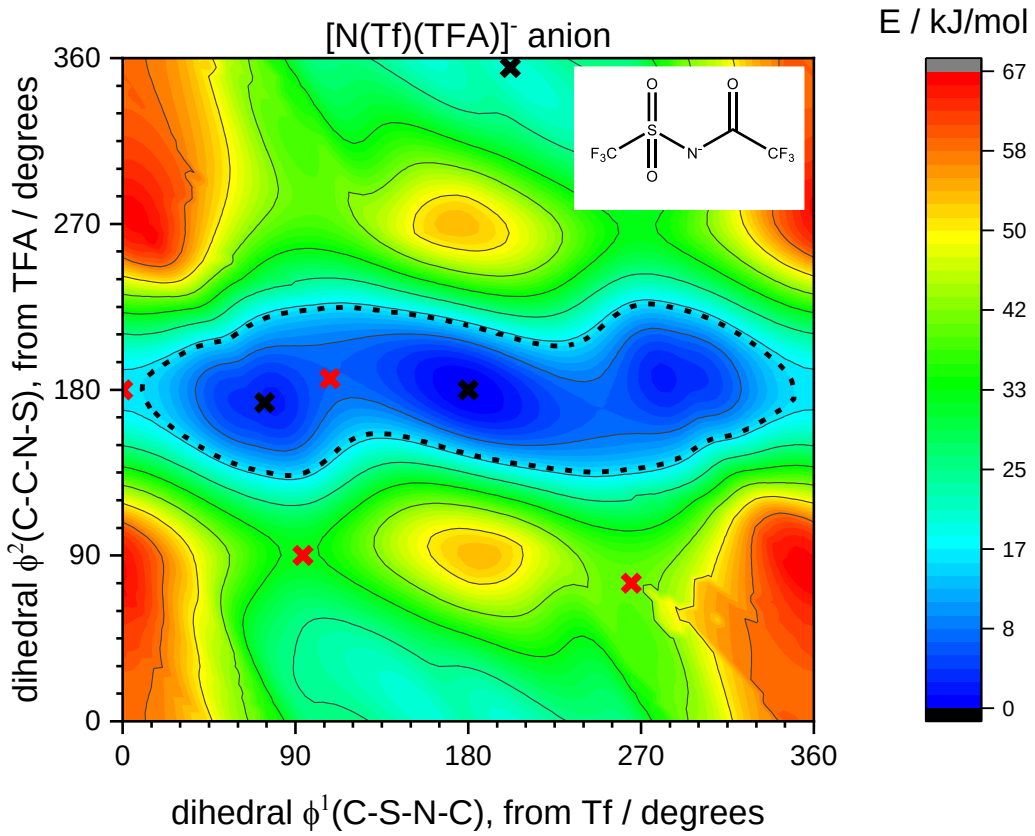

Figure 20: Potential Energy Surface of the [N(Tf)(TFA)]⁻ anion.

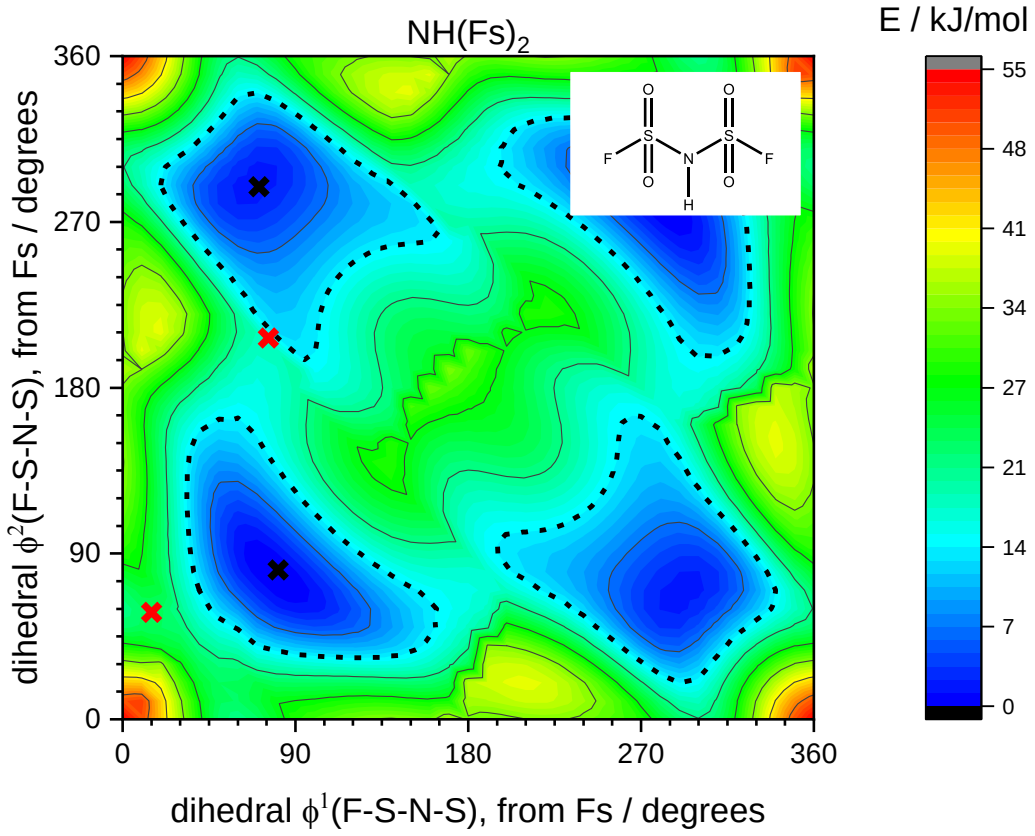

Figure 21: Potential Energy Surface of the $NH(Fs)_2$ neutral analogue.

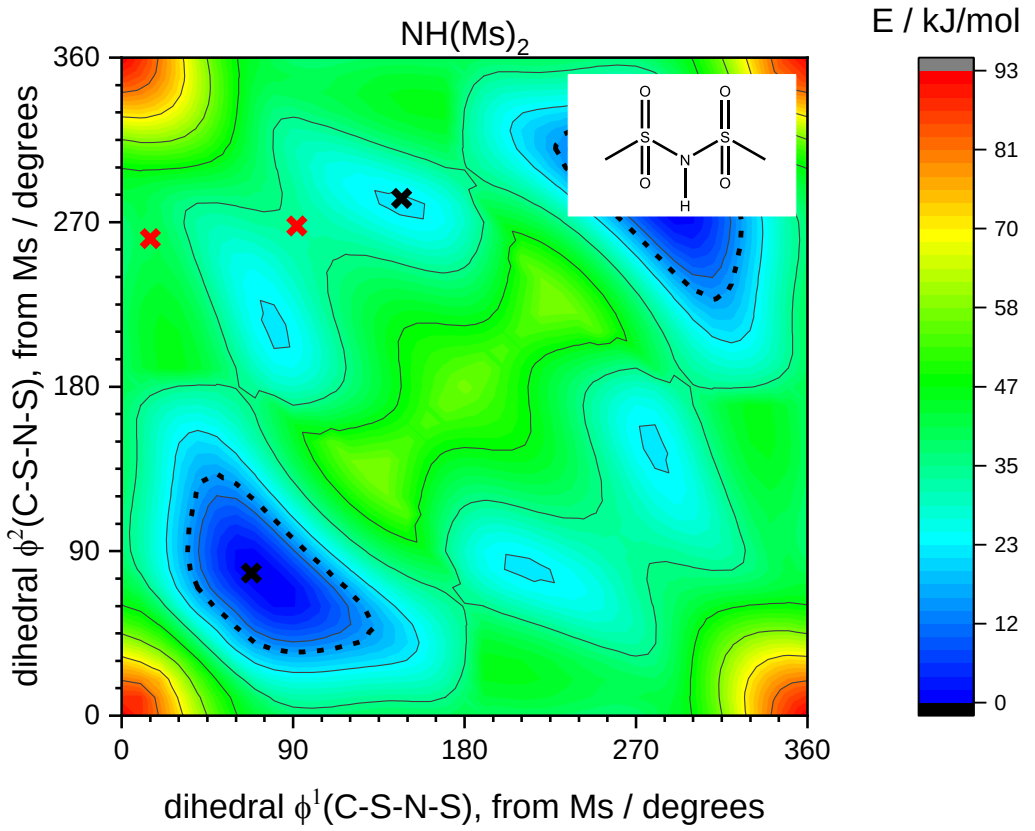

Figure 22: Potential Energy Surface of the NH(Ms)$_2$ neutral analogue.

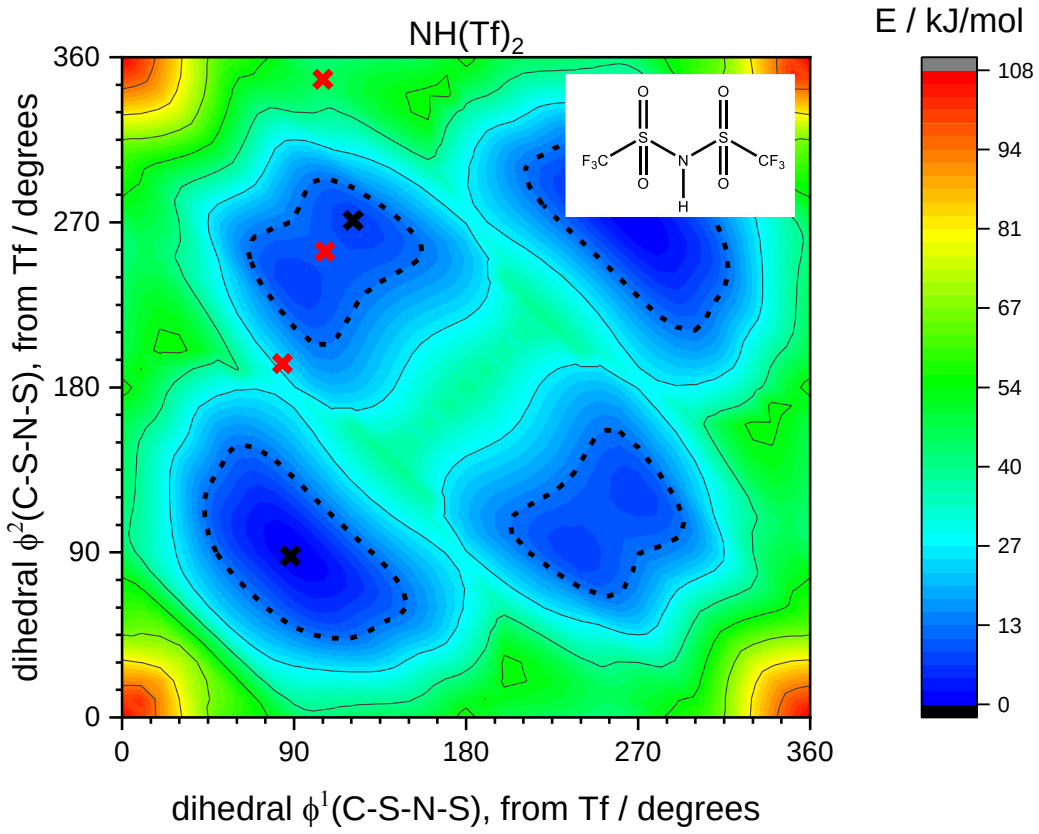

Figure 23: Potential Energy Surface of the NH(Tf)$_2$ neutral analogue.

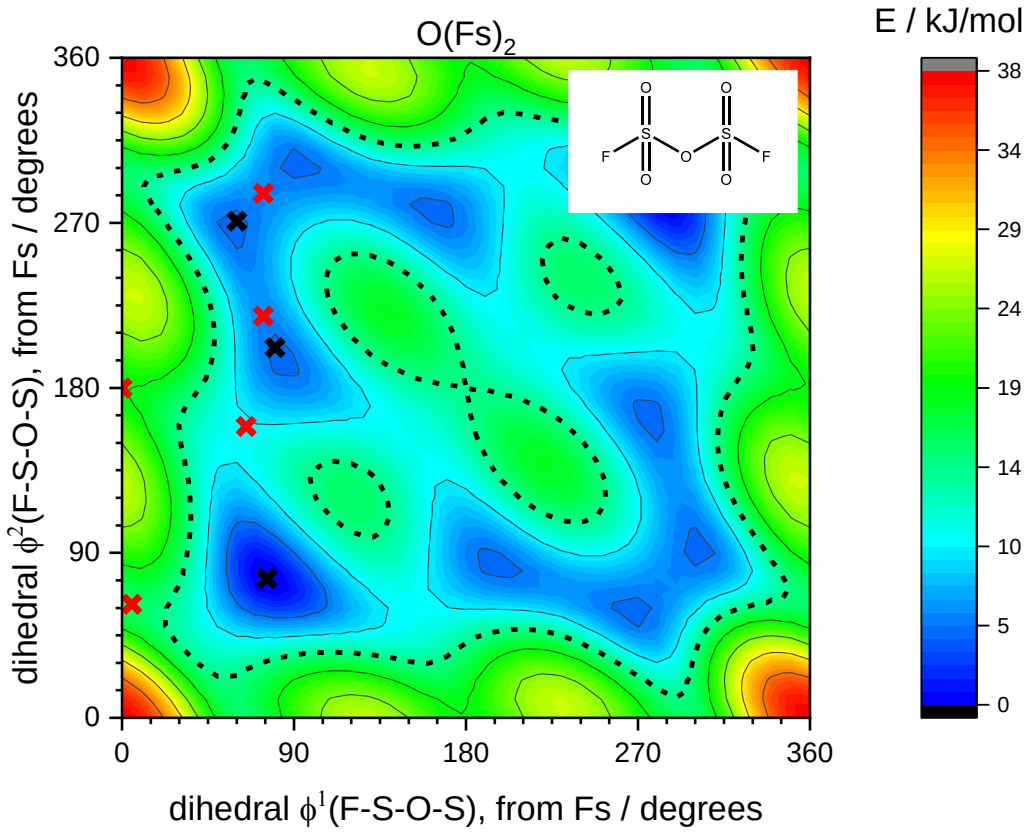

Figure 24: Potential Energy Surface of the $O(Fs)_2$ neutral analogue.

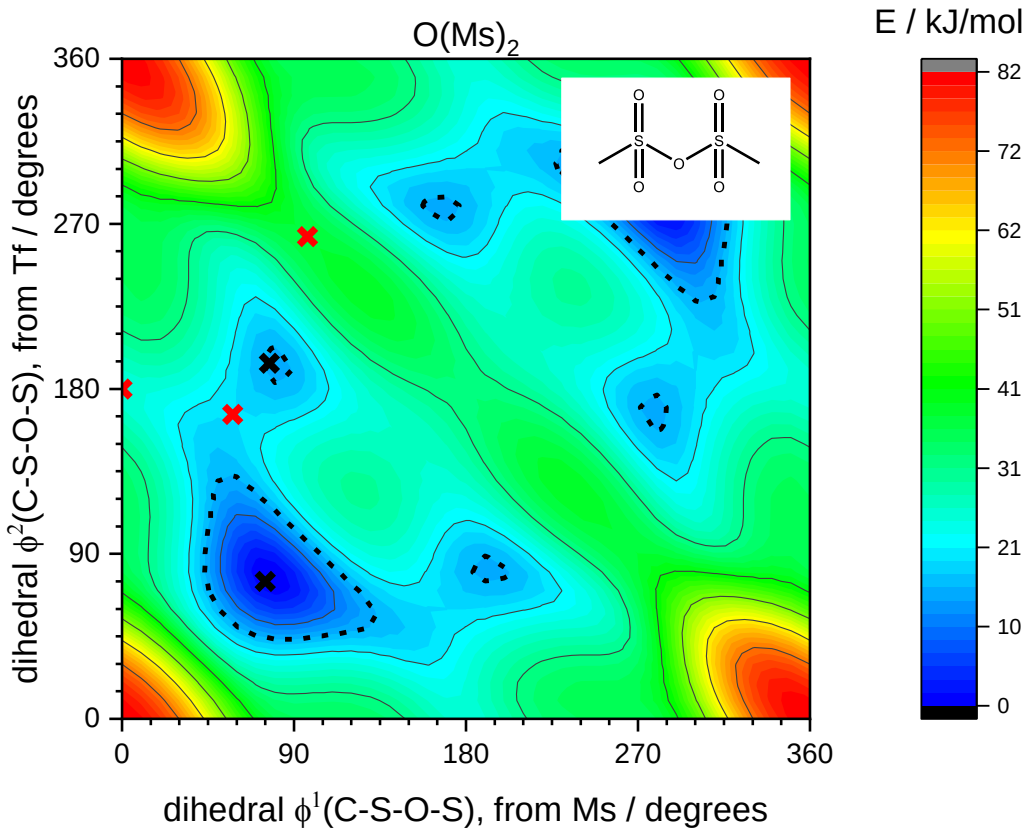

Figure 25: Potential Energy Surface of the $O(Ms)_2$ neutral analogue.

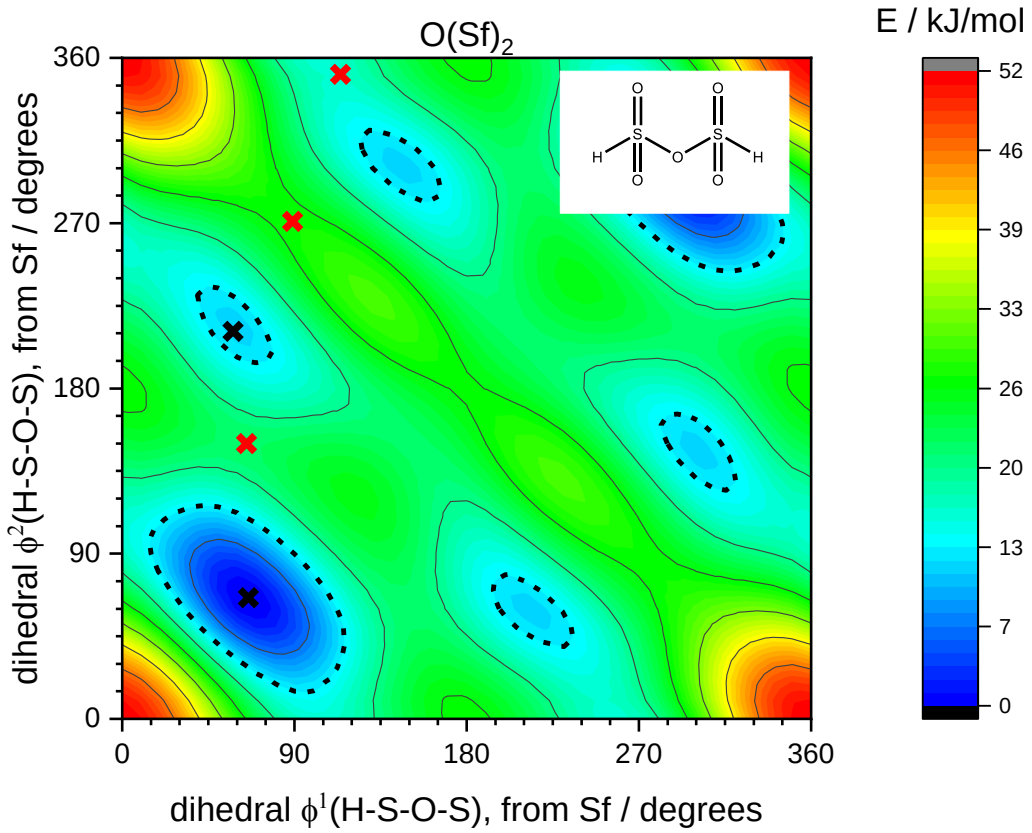

Figure 26: Potential Energy Surface of the $O(Sf)_2$ neutral analogue.

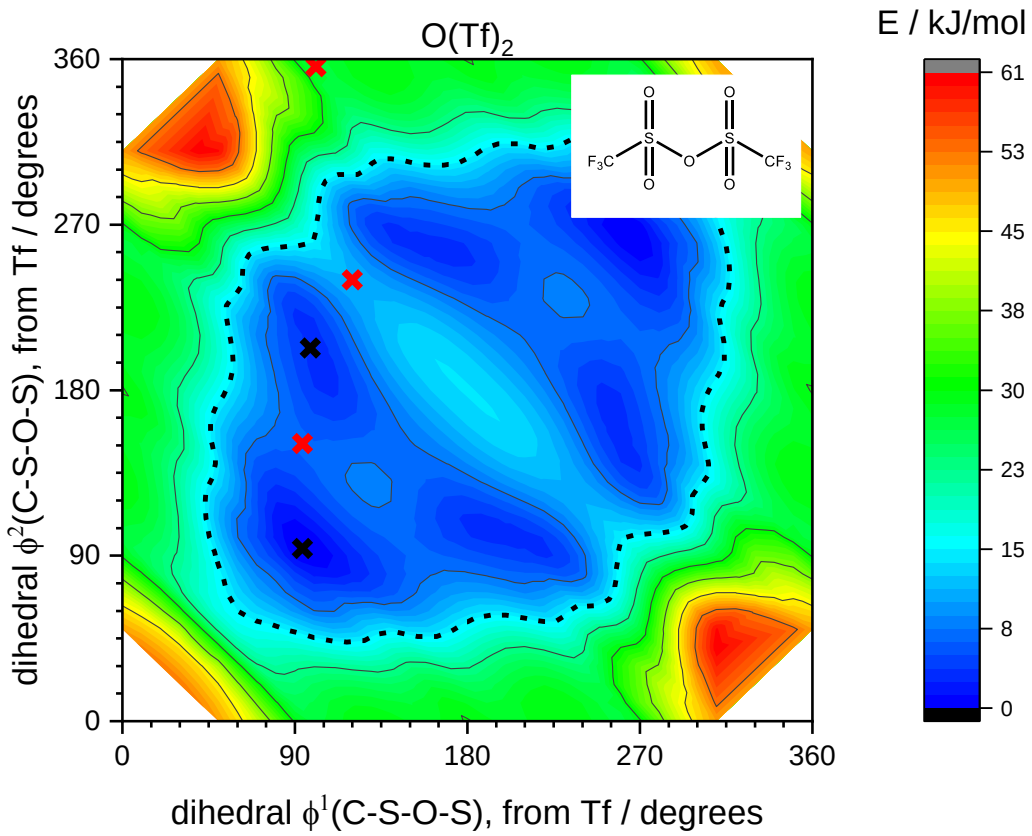

Figure 27: Potential Energy Surface of the $O(Tf)_2$ neutral analogue.

10. NMR spectra of neat ILs

NMR diffusometry was be performed on neat, dried samples with external reference. The recorded NMR spectra, Figure 28-33, are thus very sensitive to impurities. Furthermore, we provide the raw data for these samples in the folders 'BMIMMsNTFA' and 'BMIMTfNAc' accompanying this supporting information.

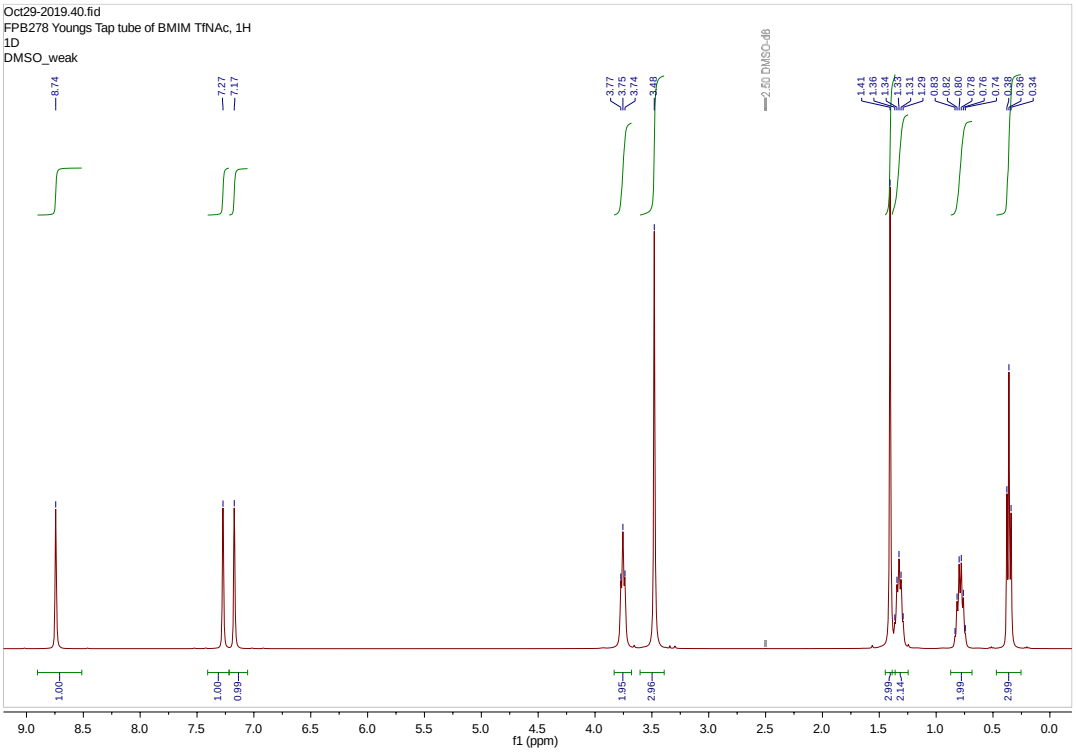

Figure 28: Proton NMR spectrum of neat [C_4C_1Im][N(Tf)(Ac)]

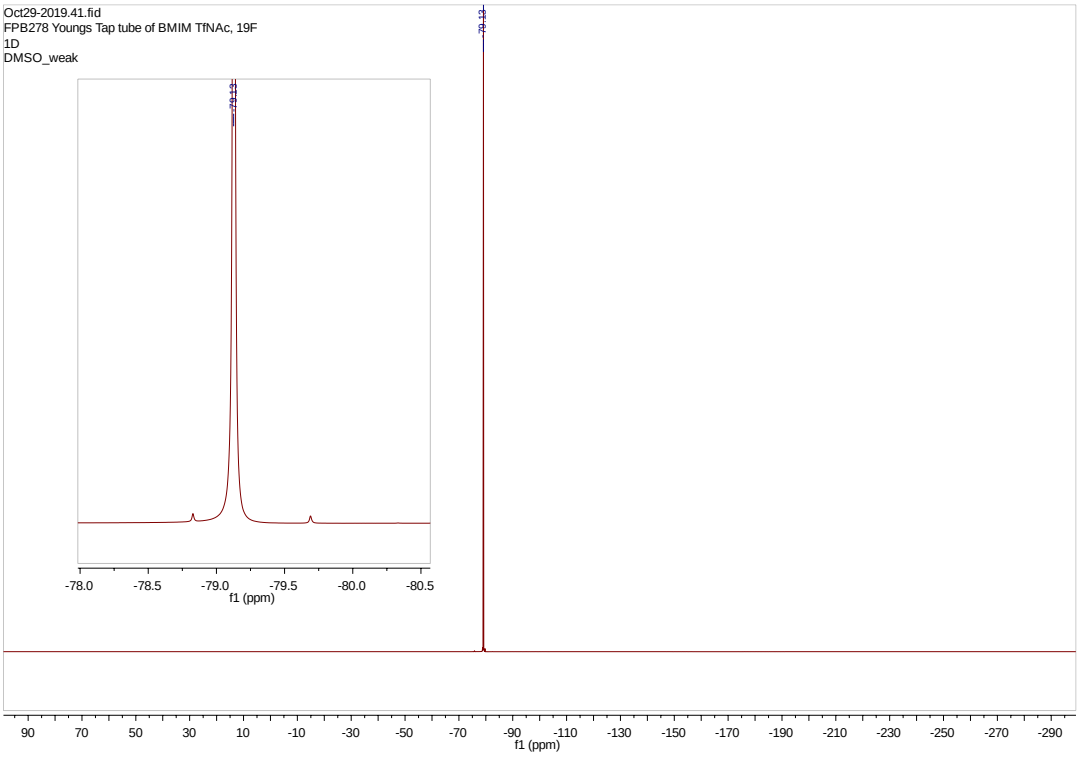

Figure 29: Fluorine NMR spectrum of neat [C_4C_1Im][N(Tf)(Ac)]

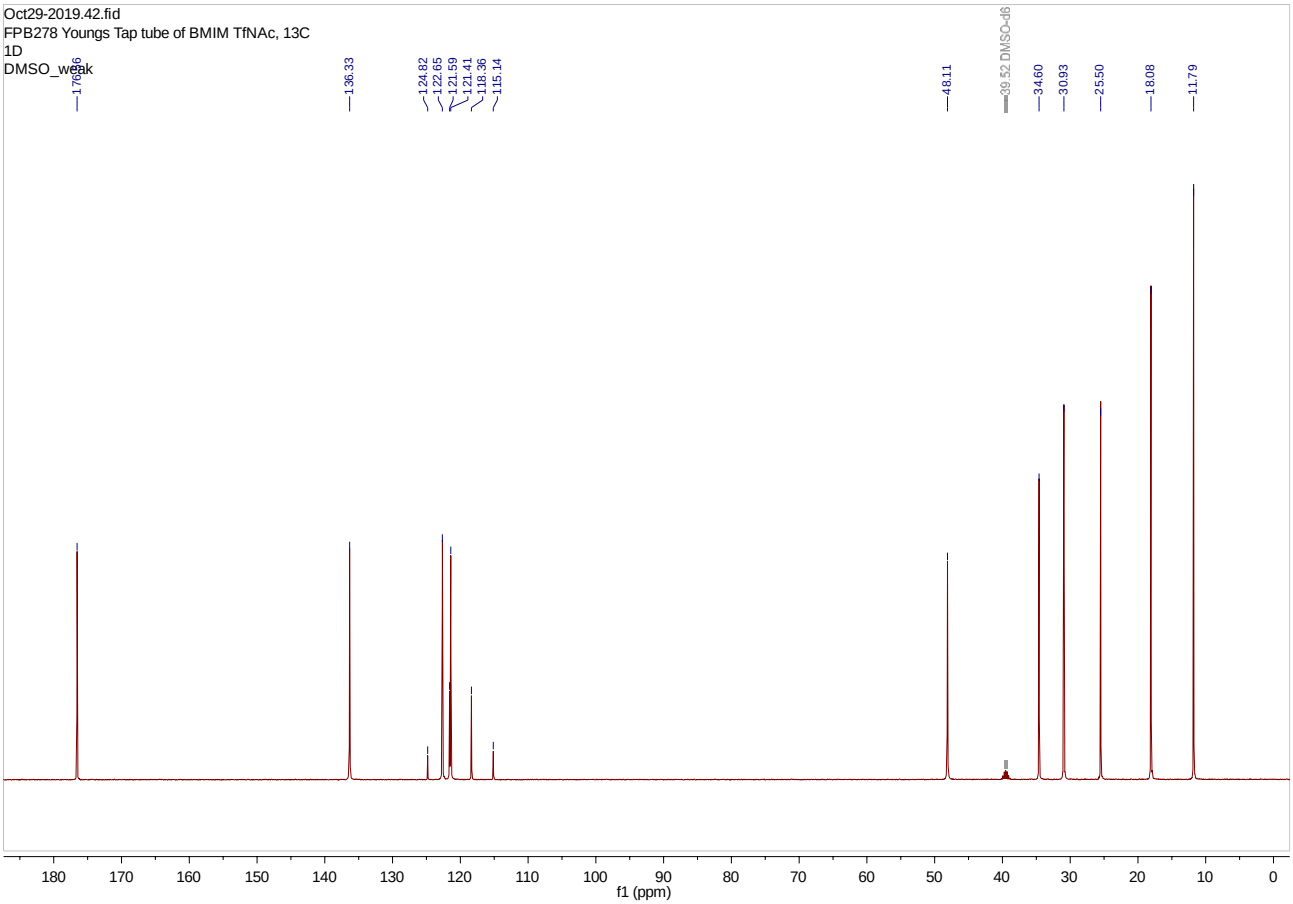

Figure 30: Carbon NMR spectrum of neat [C_4C_1Im][N(Tf)(Ac)]

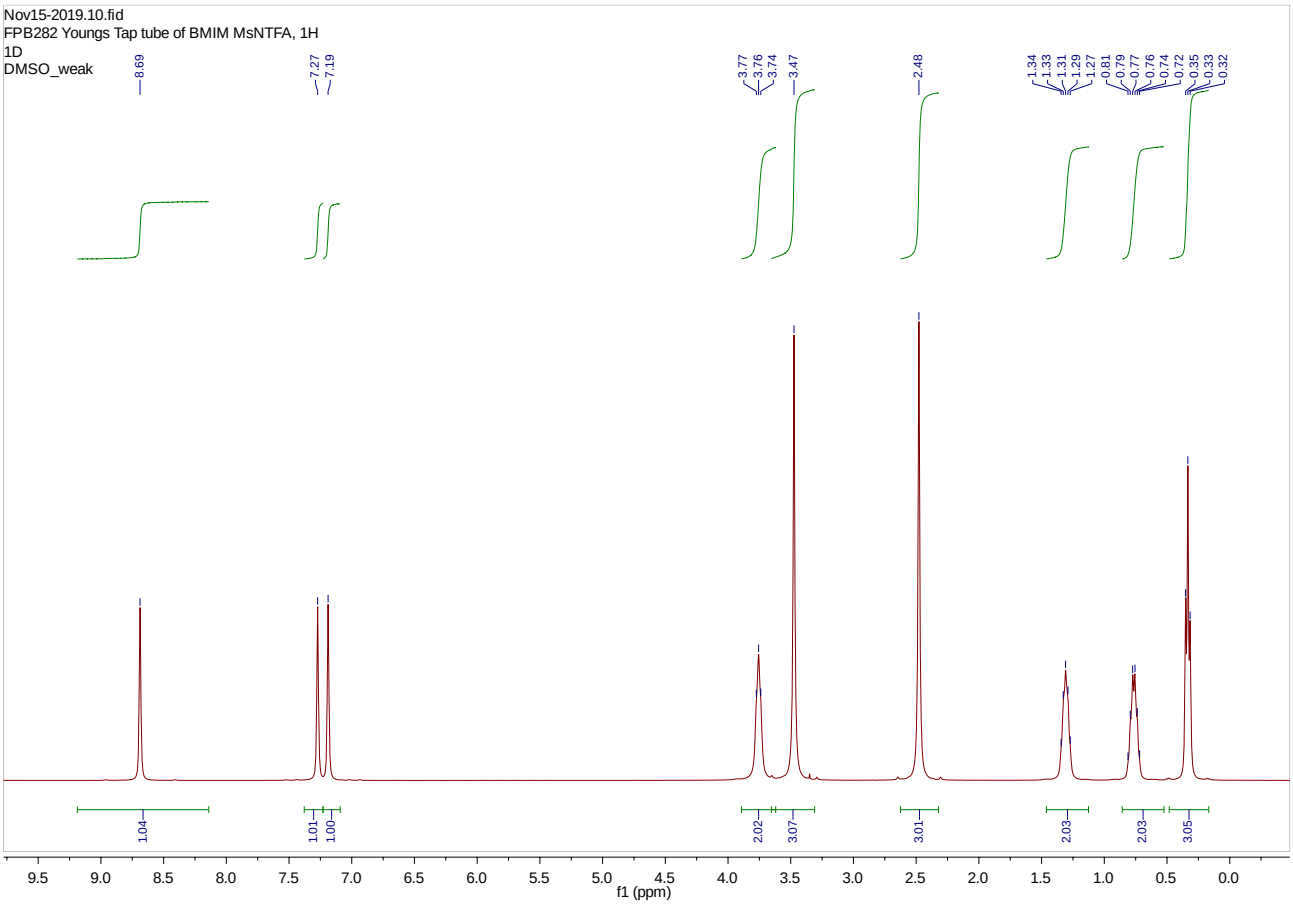

Figure 31: Proton NMR spectrum of neat [C_4C_1Im][N(Ms)(TFA)]

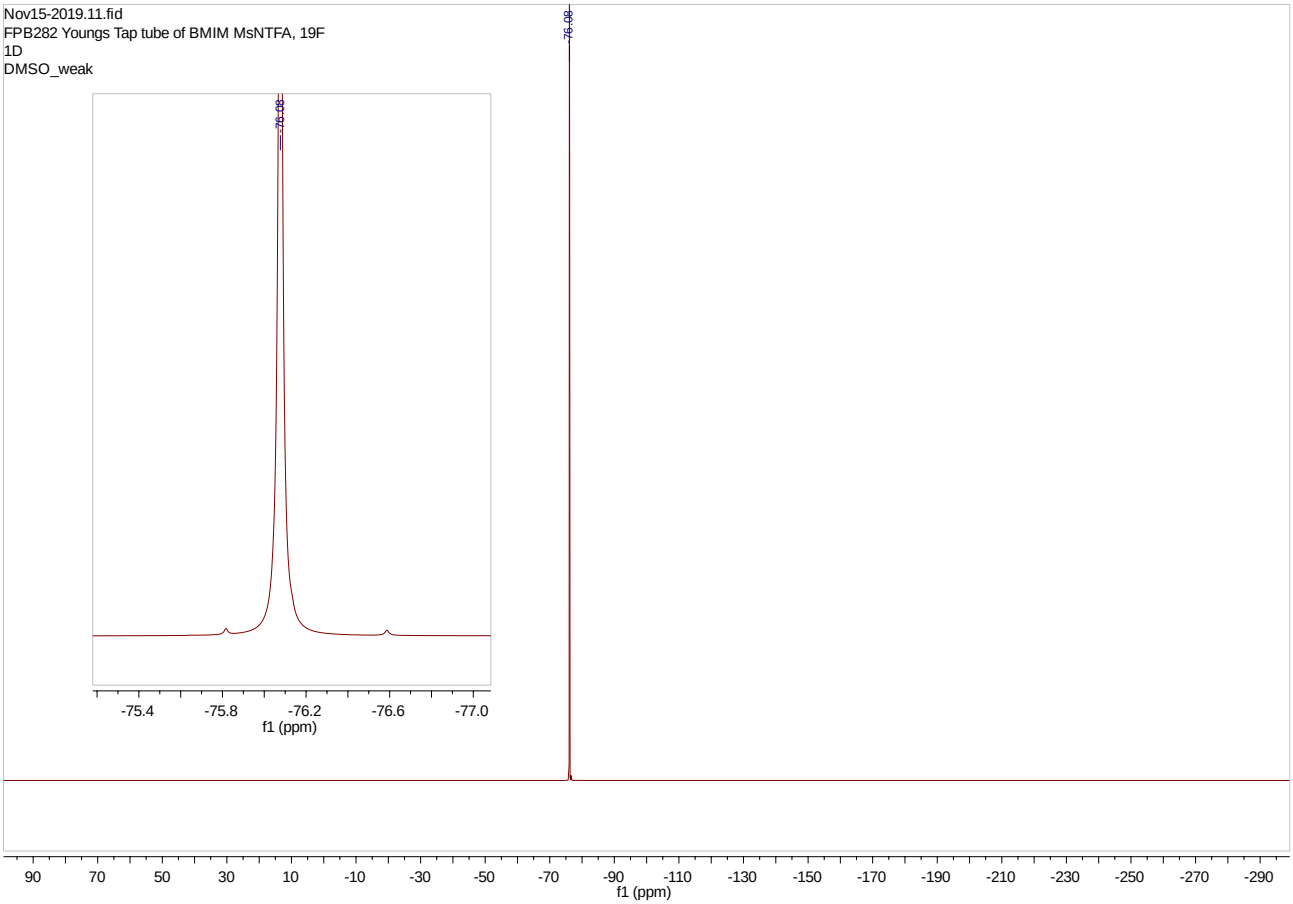

Figure 32: Fluorine NMR spectrum of neat [C_4C_1Im][N(Ms)(TFA)]

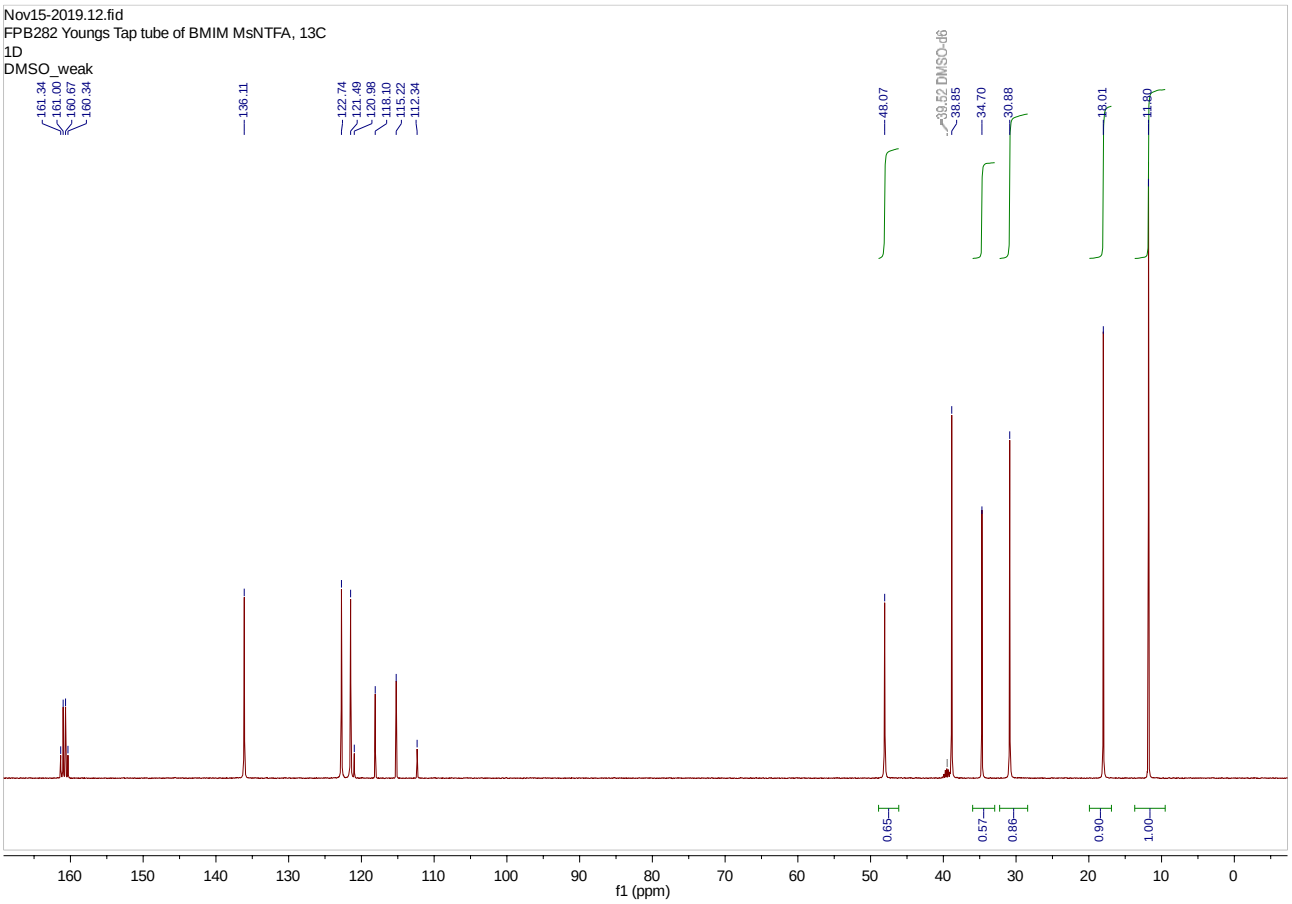

Figure 33: Carbon NMR spectrum of neat [C_4C_1Im][N(Ms)(TFA)]

11. NMR spectra of precursors

NMR spectra of the precursors [H][N(Tf)(Ac)] (Figure 34 – Figure 36), [Na][N(Tf)(Ac)] (Figure 37 – Figure 39), [H][N(Ms)(TFA)] (Figure 40 – Figure 42) and [Na][N(Ms)(TFA)] (Figure 43 – Figure 45) are given below.

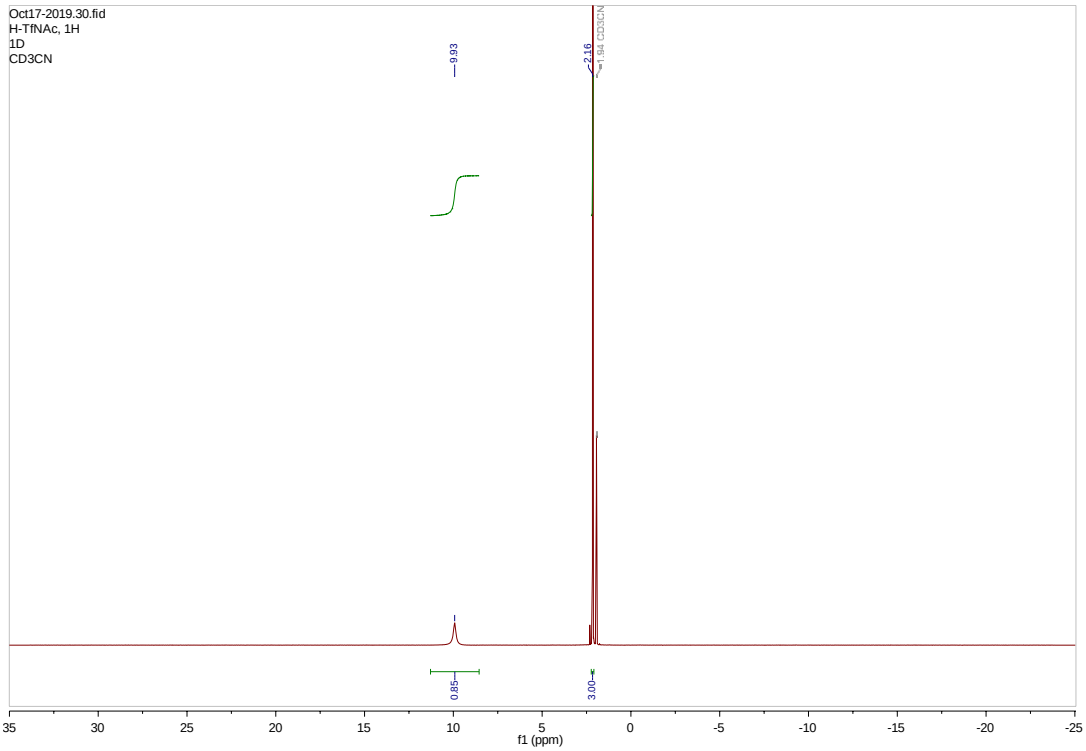

Figure 34: Proton NMR spectrum of [H][N(Tf)(Ac)].

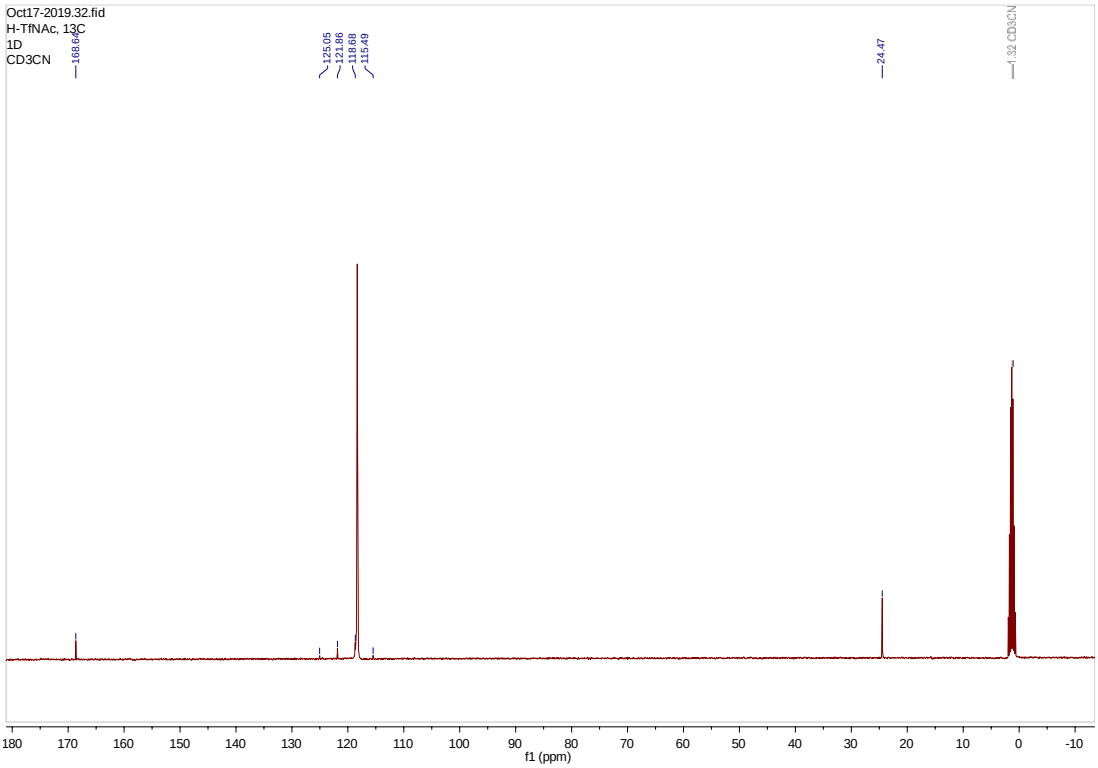

Figure 35: Carbon NMR spectrum of [H][N(Tf)(Ac)].

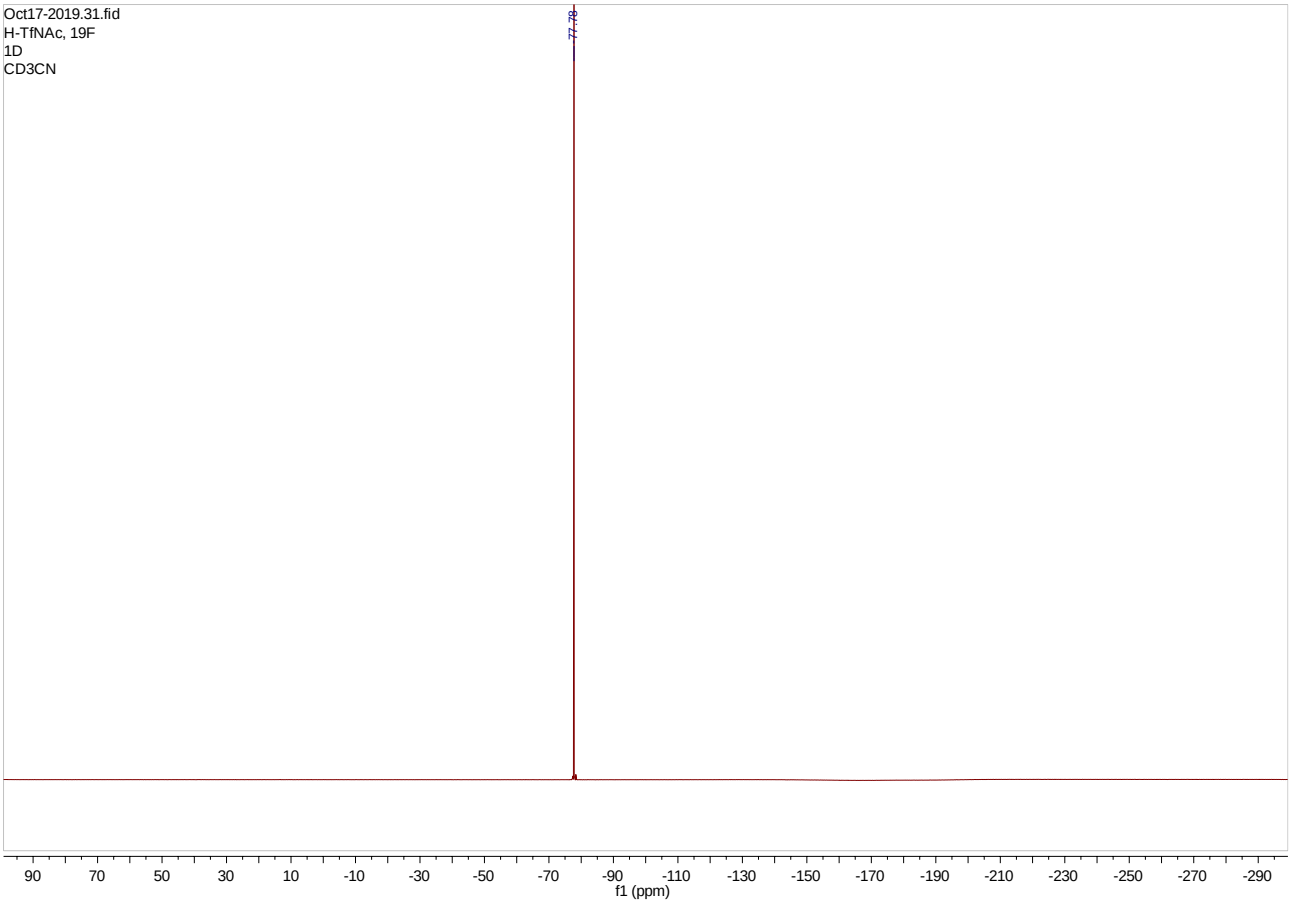

Figure 36: Fluorine NMR spectrum of [H][N(Tf)(Ac)].

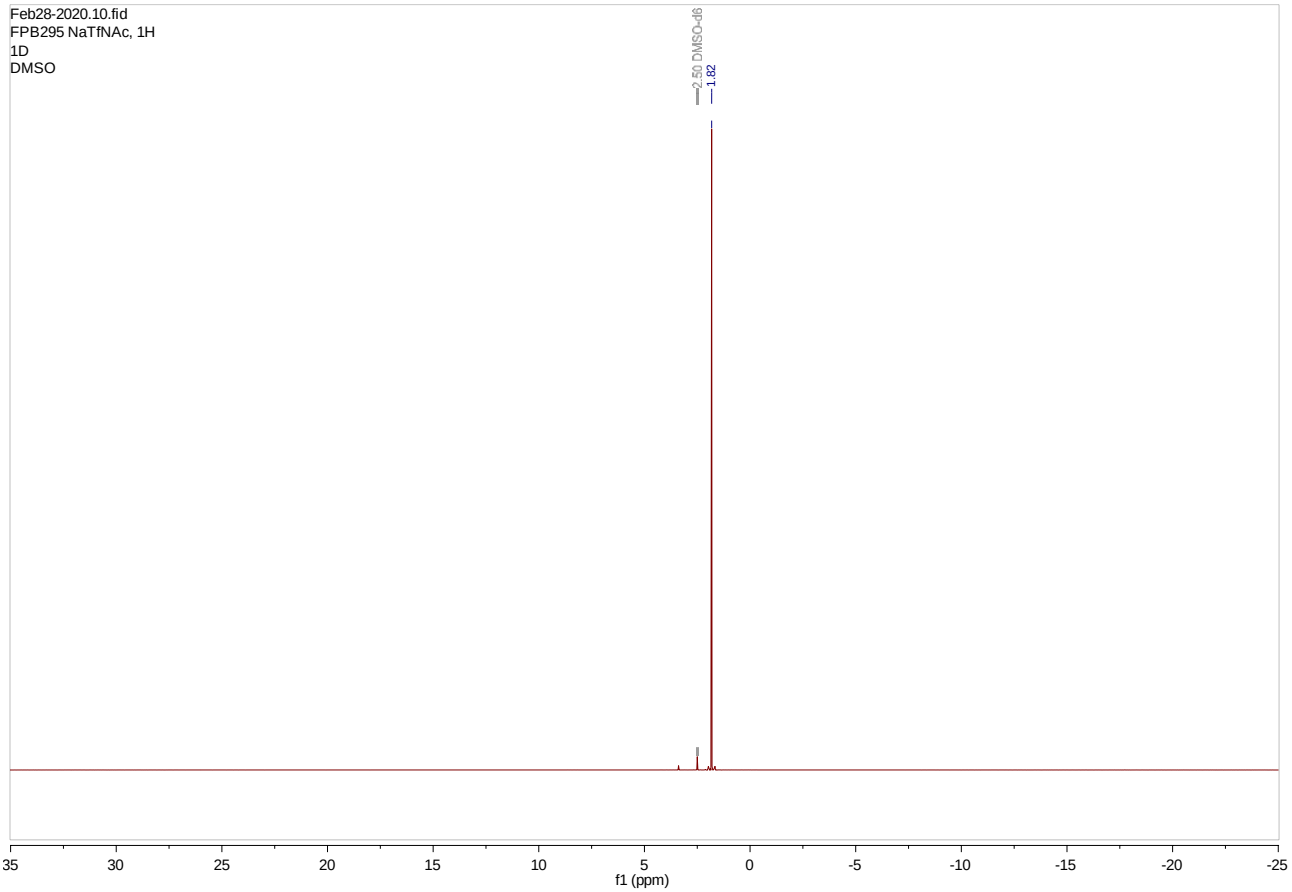

Figure 37: Proton NMR spectrum of [Na][N(Tf)(Ac)].

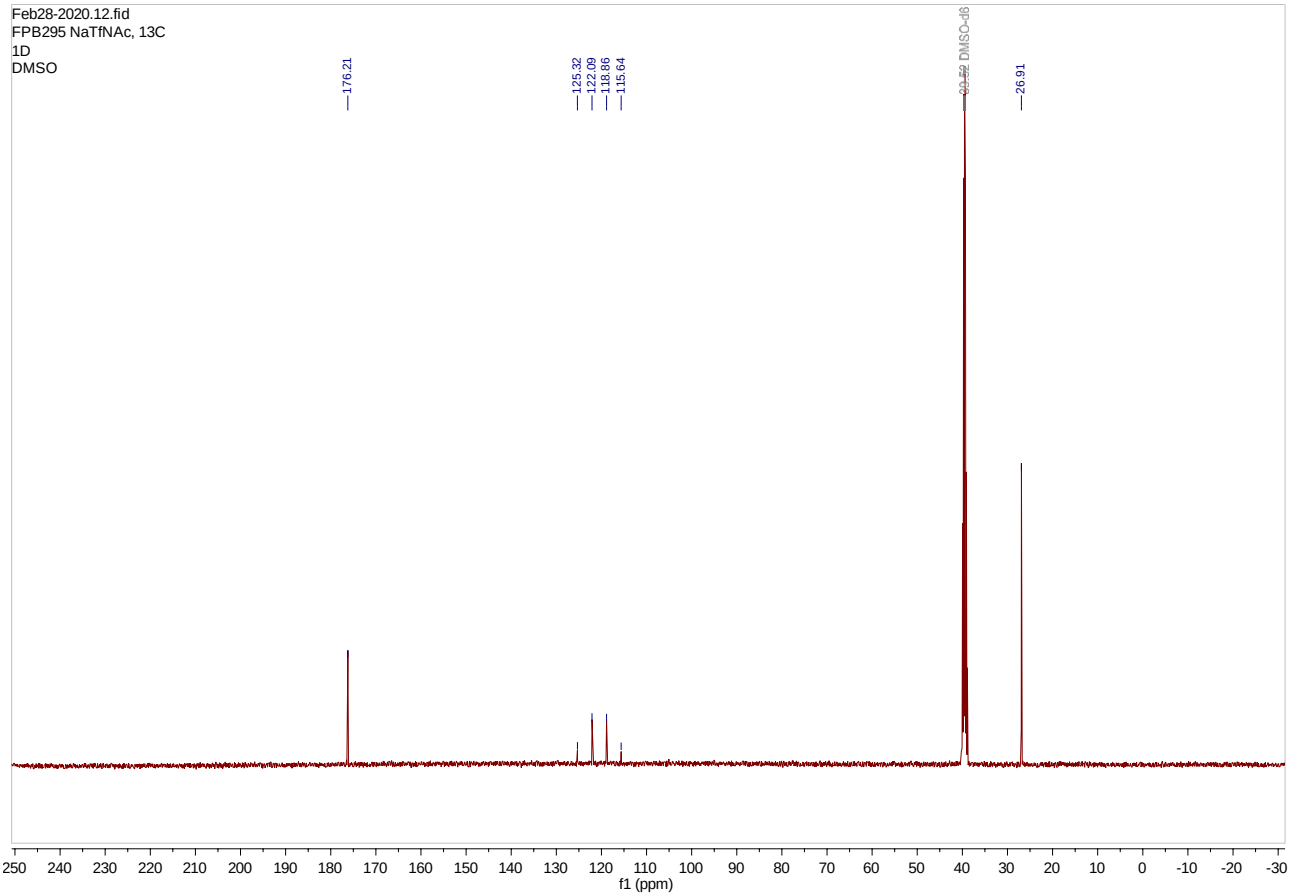

Figure 38: Carbon NMR spectrum of [Na][N(Tf)(Ac)].

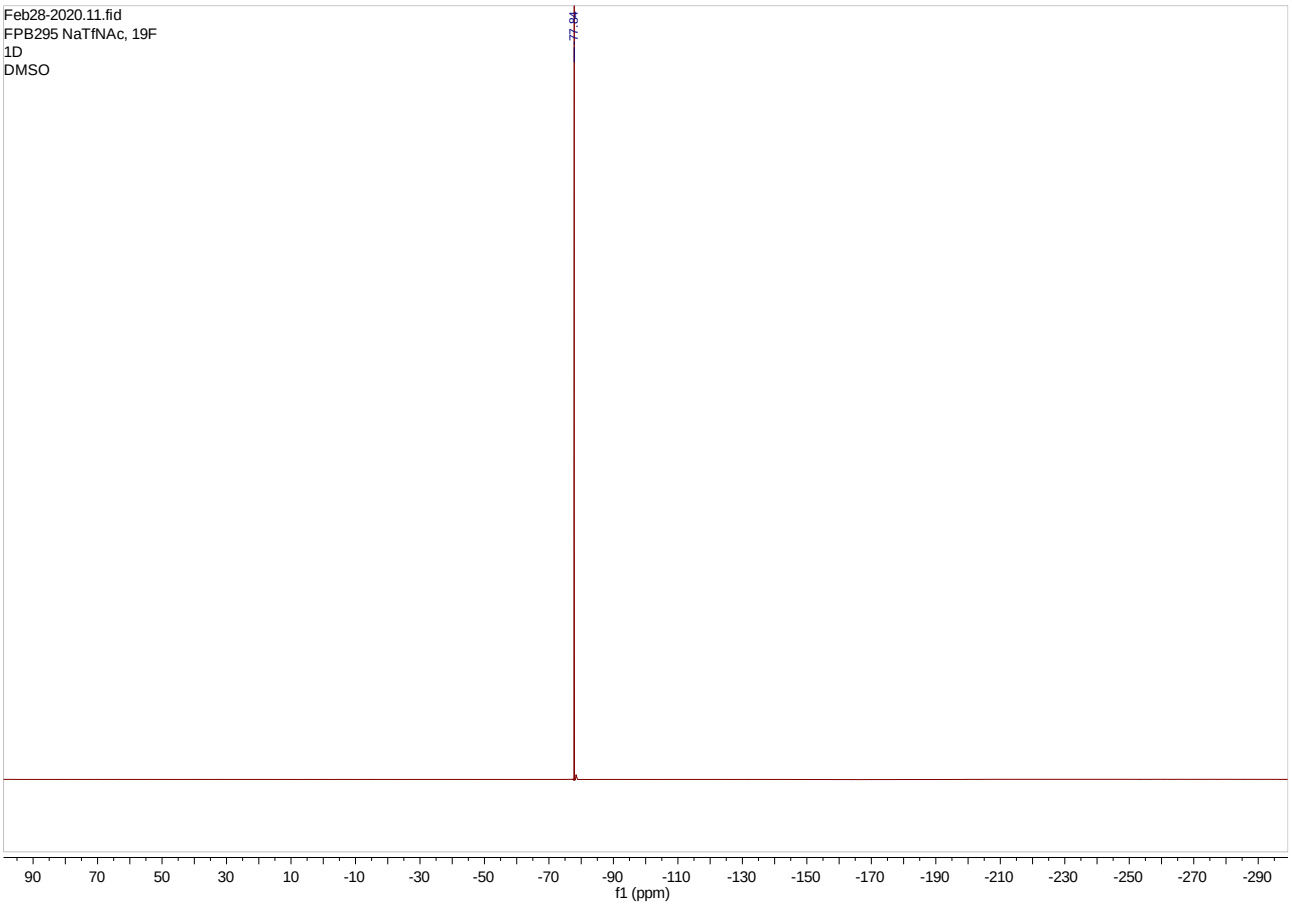

Figure 39: Fluorine NMR spectrum of [Na][N(Tf)(Ac)].

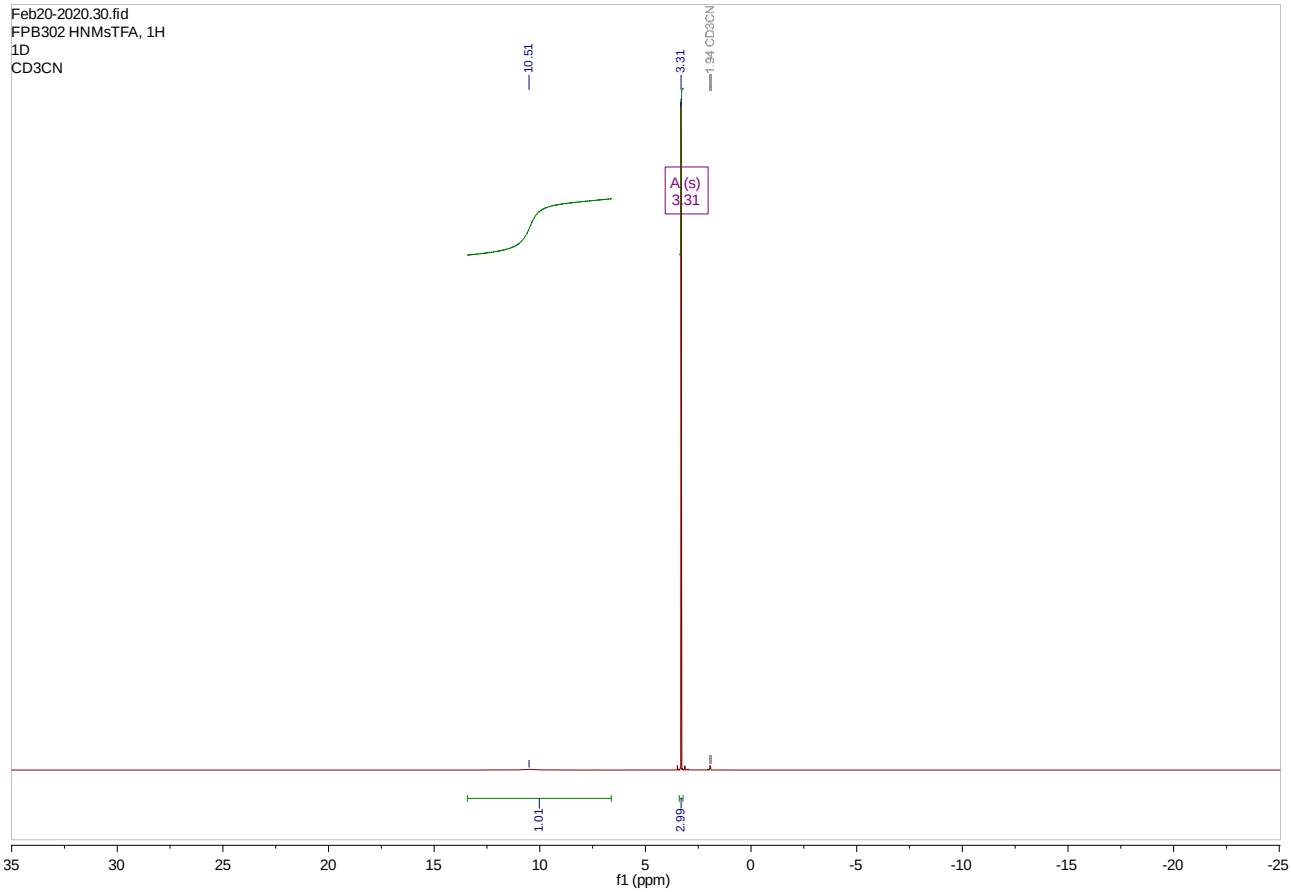

Figure 40: Proton NMR spectrum of [H][N(Ms)(TFA)].

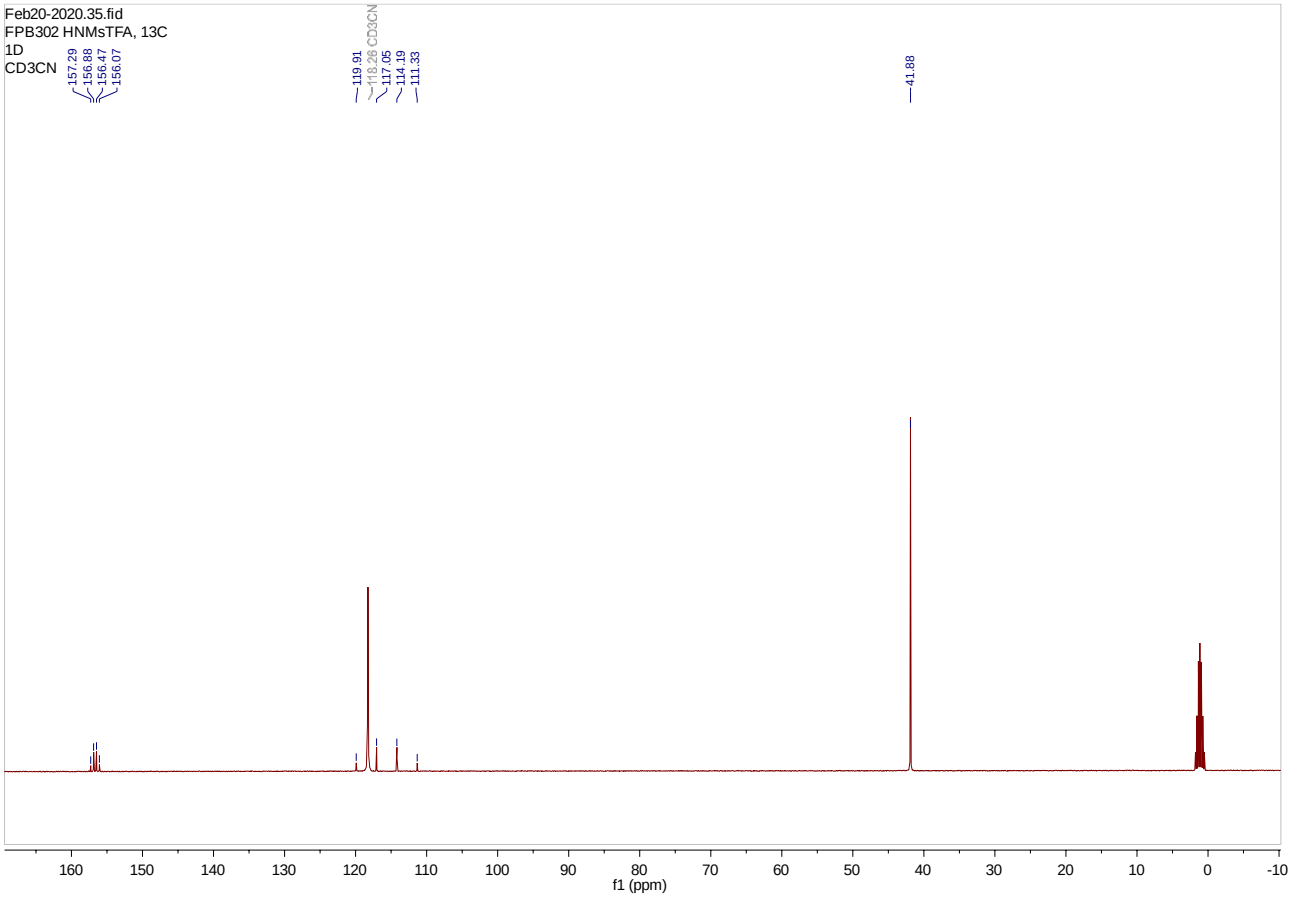

Figure 41: Carbon NMR spectrum of [H][N(Ms)(TFA)].

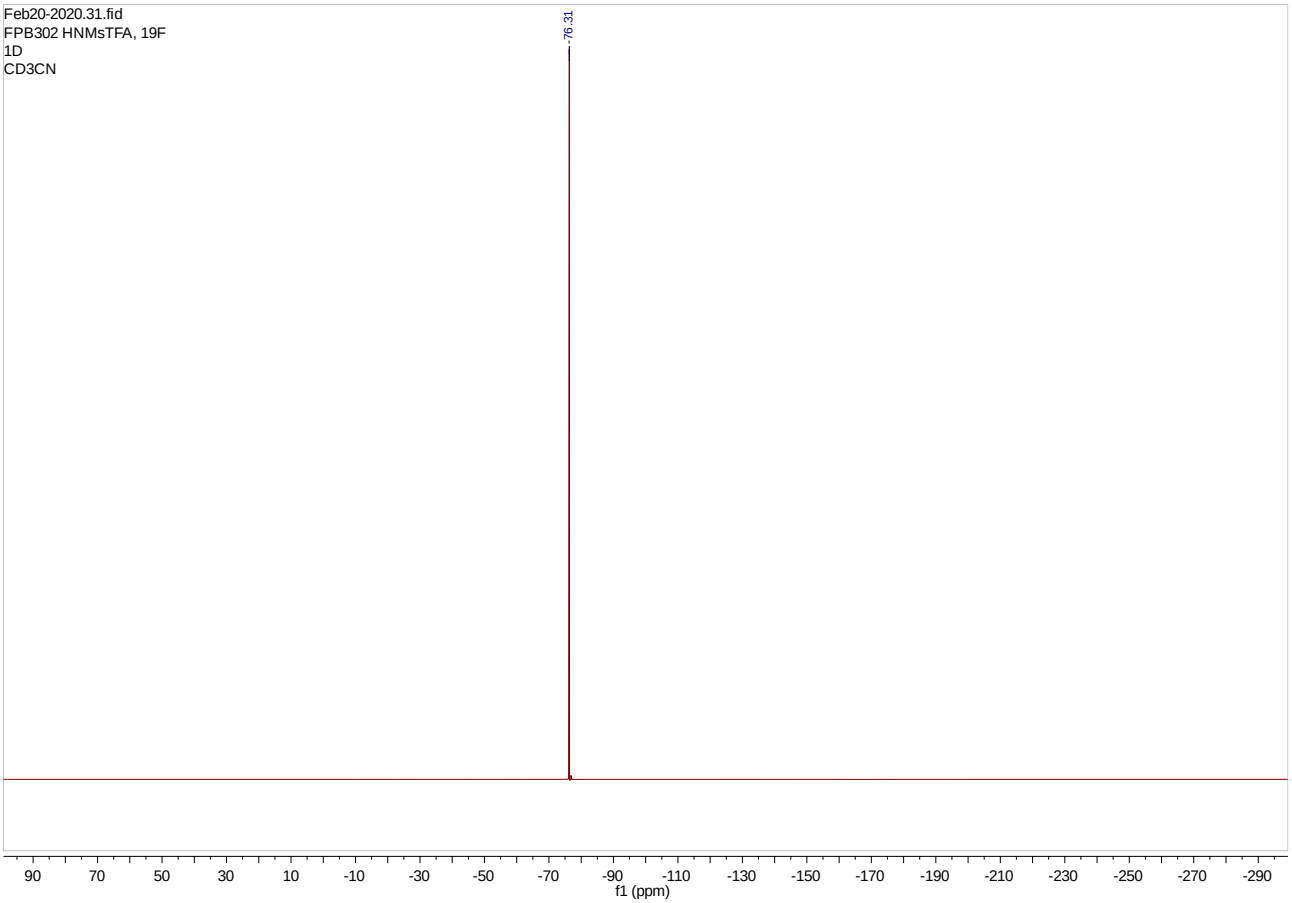

Figure 42: Fluorine NMR spectrum of [H][N(Ms)(TFA)].

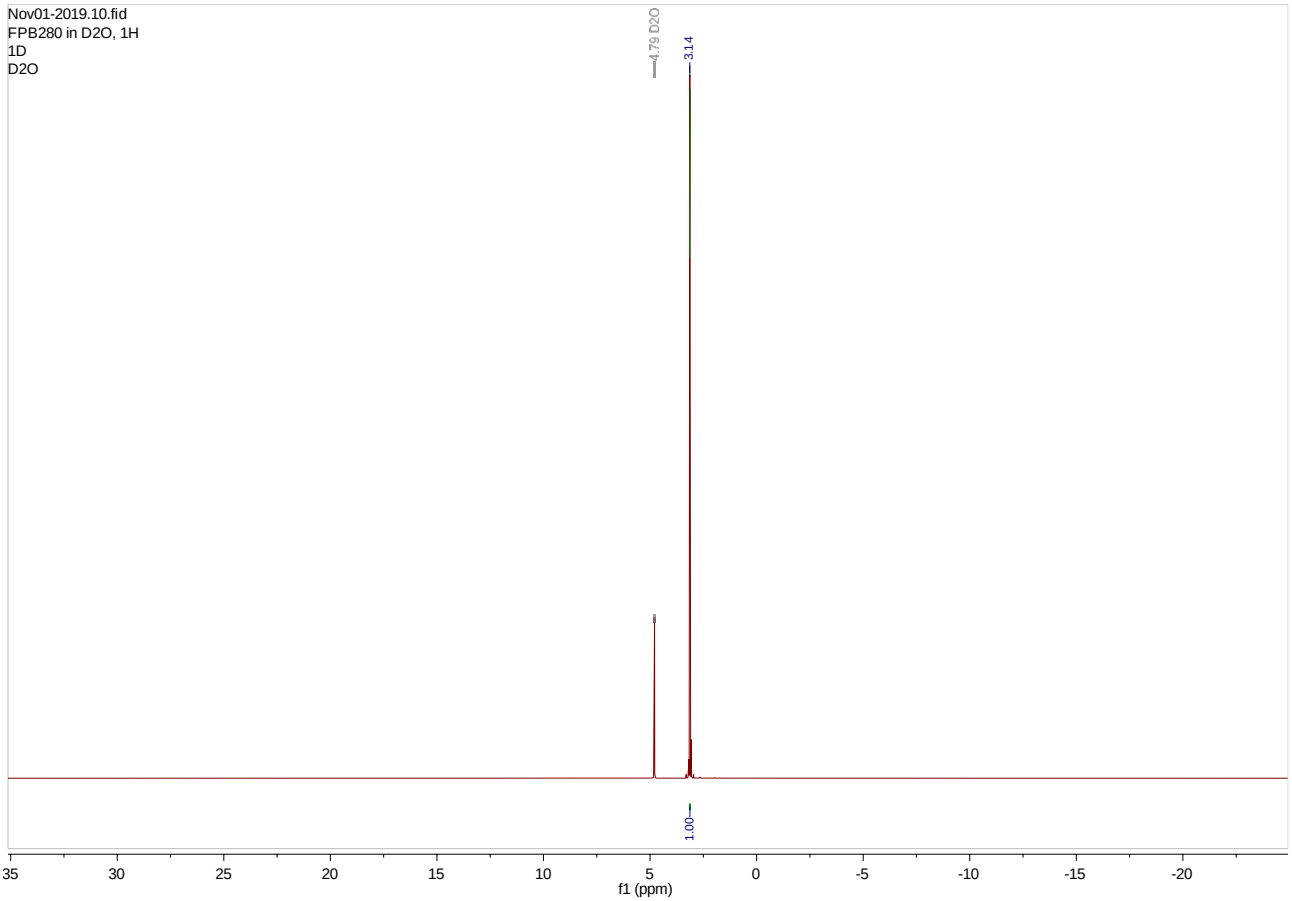

Figure 43: Proton NMR spectrum of [Na][N(Ms)(TFA)].

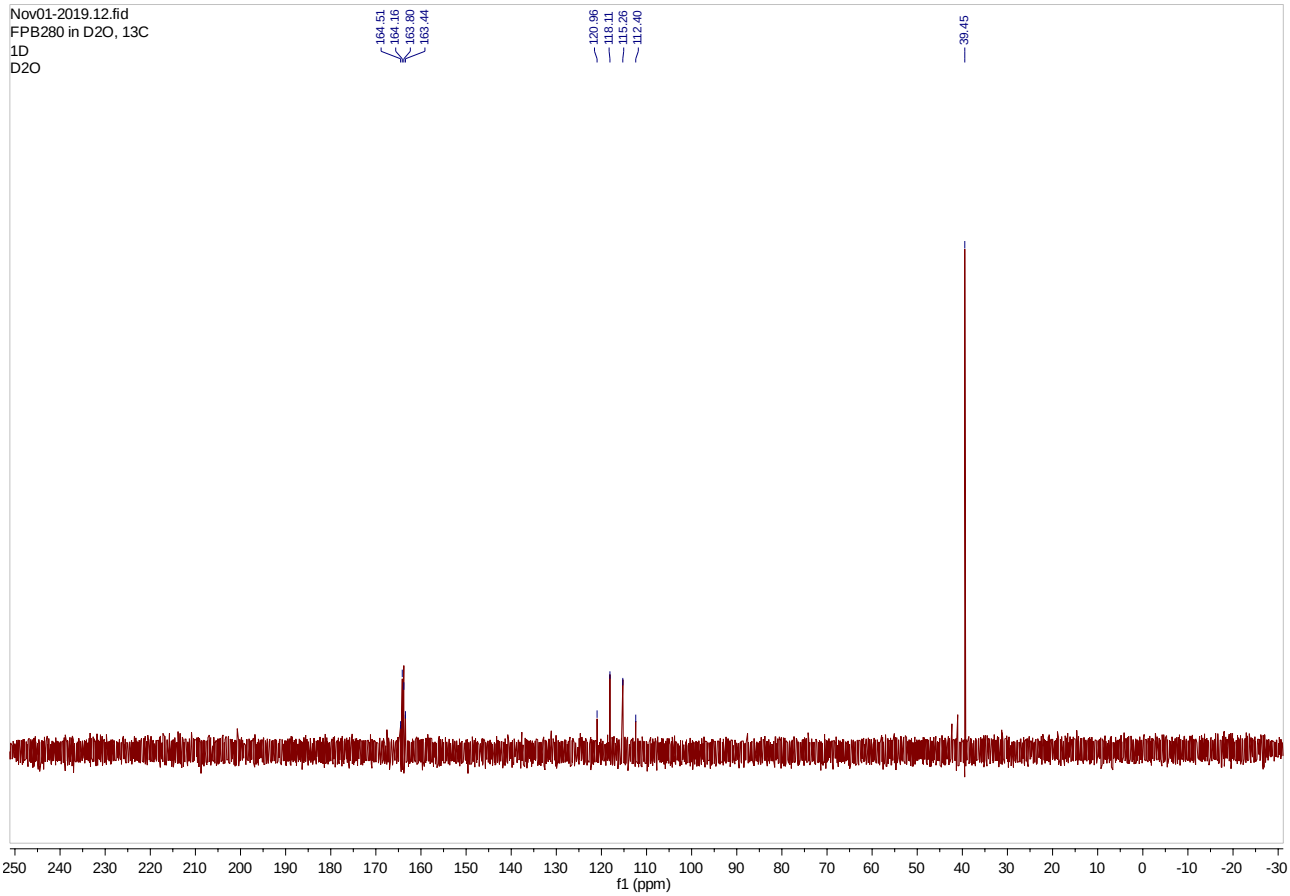

Figure 44: Carbon NMR spectrum of [Na][N(Ms)(TFA)].

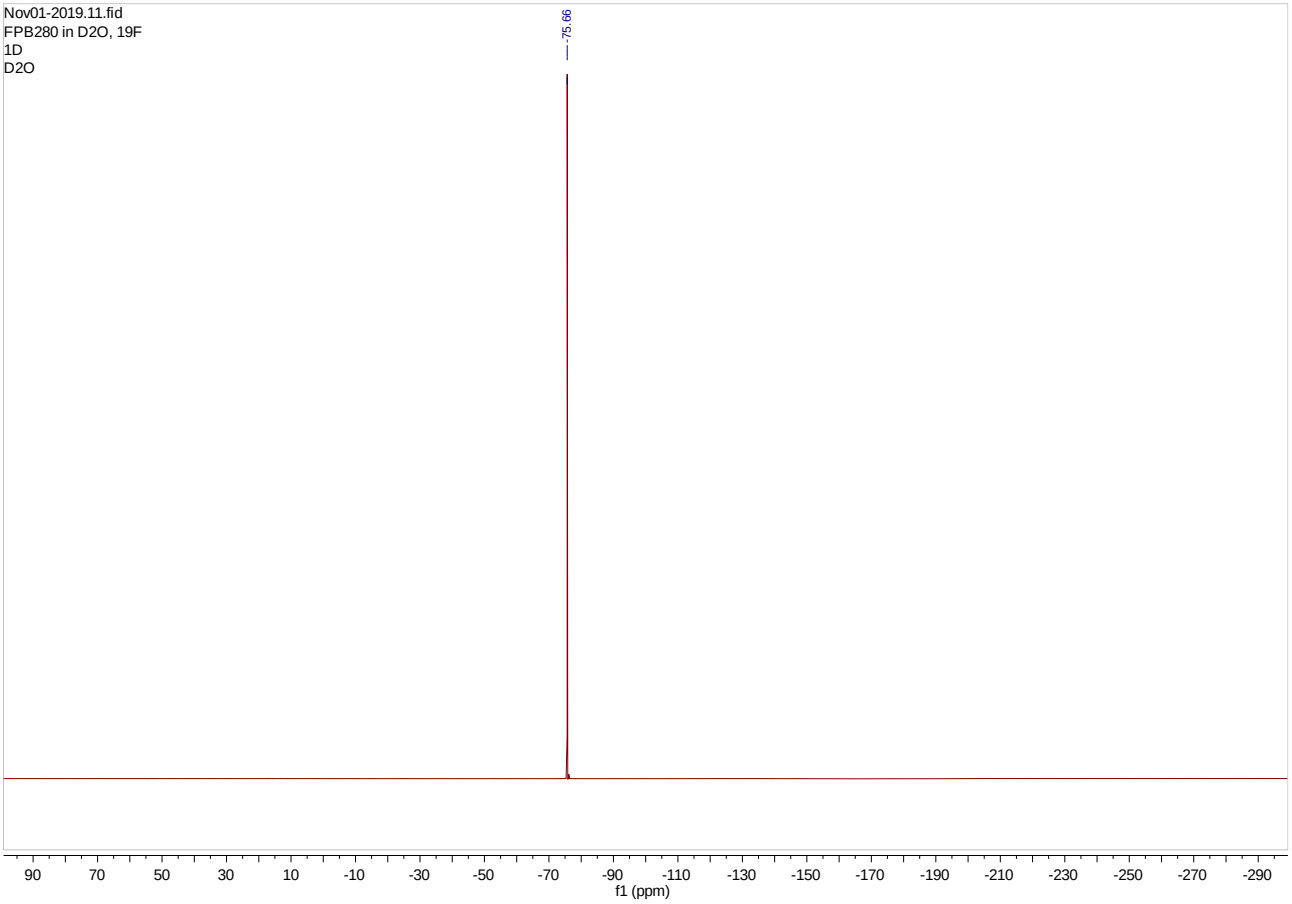

Figure 45: Fluorine NMR spectrum of [Na][N(Ms)(TFA)].

12. References

1) Martin, M. T.; Roschanger, F.; Eaddy, J. F. Practical acid-catalyzed acylation of sulfonamides with carboxylic acid anhydrides. *Tetrahedron Lett.*, **2003**, *44*, 5461-5463.

2) CrysAlis Pro: Agilent, **2014**, Agilent Technologies Ltd, Yarnton, Oxfordshire, UK.

3) Sheldrick, G. M. A short history of SHELX. *Acta Crystallogr. Sect. A*, **2008**, *64*, 112.

4) Dolomanov, O. V.; Bourhis, L. J.; Gildea, R. J.; Howard, J. A. K.; Puschmann, H. OLEX2: a complete structure solution, refinement and analysis program. *J. Appl. Cryst.*, **2009**, *42*, 339.

5) Farrugia, L. J. WinGX and ORTEP for Windows: an update. *J. Appl. Cryst.*, **2012**, *45*, 849.

6) G. S. Fulcher, ANALYSIS OF RECENT MEASUREMENTS OF THE VISCOSITY OF GLASSES, *J. Am. Ceram. Soc.*, **1925**, 8, 339–355.

7) G. Tammann, W. Hesse, Die Abhängigkeit der Viscosität von der Temperatur bei unterkühlten Flüssigkeiten, *Zeitschrift für Anorg. und Allg. Chemie*., **1926**, 156, 245–257.

8) H. Tokuda, K. Hayamizu, K. Ishii, M. A. B. H. Susan, M. Watanabe, Physicochemical Properties and Structures of Room Temperature Ionic Liquids. 1. Variation of Anionic Species, *J. Phys. Chem. B*., **2004**, 108, 16593–16600.

9) O. Zech, A. Stoppa, R. Buchner, W. Kunz, The Conductivity of Imidazolium-Based Ionic Liquids from (248 to 468) K. B. Variation of the Anion †, *J. Chem. Eng. Data*., **2010**, 55, 1774–1778.

10) H. Tokuda, K. Hayamizu, K. Ishii, M. A. B. H. Susan, M. Watanabe, Physicochemical Properties and Structures of Room Temperature Ionic Liquids. 2. Variation of Alkyl Chain Length in Imidazolium Cation, *J. Phys. Chem. B*., **2005**, 109, 6103–6110.